Linking travel times and flow pathways to stream chemistry, isotopic composition, and catchment characteristics in a boreal landscape

Elin Jutebring Sterte[1,2], Fredrik Lidman[1], Emma Lindborg[2], Ylva Sjöberg[3], Hjalmar Laudon[1]

[1]Department of Forest Ecology and Management, Swedish University of Agricultural Sciences, SE-901 83 Umeå, SWEDEN

[2]DHI Sweden AB, Skeppsbron 28, SE- 111 30 Stockholm, SWEDEN

[3]Center for Permafrost (CENPERM), Department of Geosciences and Natural Resource Management, University of Copenhagen, Øster Voldgade 10, 1350 Copenhagen, Denmark

Corresponding author: Elin Jutebring Sterte (eljs@dhigroup.com)

Key Points:

- A numerical model was used to estimate annual and seasonal mean travel times across 14 long-term monitored sub-catchment in the boreal region of northern Sweden.
- The estimated travel times and young water fractions were consistent with observed variations of base cation concentration and stable water isotopes, $\delta^{18}O$.
- The soil type was the most important factor regulating the variation in mean travel times between different sub-catchments, while the areal coverage of mires affected the young water fraction.
- The greatest seasonality in mean travel times was found in sub-catchments dominated by silty soils contributing with old water during winter baseflow, while mires contributed the largest fraction young water during spring snowmelt.

Abstract

Understanding travel times and hydrological pathways of rain and snowmelt water transported through the landscape to recipient surface waters is critical in many hydrological and biogeochemical investigations. In this study, a particle tracking model approach in Mike SHE was used to investigate the travel time, and pathway of water in 14 partly nested, long-term monitored boreal sub-catchments. These sub-catchments are characterized by long and snow-rich winters with little groundwater recharge and highly dynamic runoff during spring snowmelt. The geometric mean of the travel time distribution (MTT_{geo}) for these sub-catchments varied from 0.8-2.7 years. The variations were found to be related to the distribution of different landscape types and their different response to seasonal changes. Winter MTT_{geo} ranged from 1.2-7.7 years, while spring MTT_{geo} varied between 0.5-1.9 years. The modelled variation in annual and seasonal MTT_{geo} and the fraction of young water (<3 months) was supported by extensive observations of both $\delta^{18}O$ and base cation concentrations in the different streams. The groundwater age was positively correlated to the areal coverage of low conductive silty sediments ($r=0.90$, $P<0.0001$). As a result of lacking synchronicity and contrasting hydrological responses between different soil types (e.g., mires and silty sediments), mixed catchments typically displayed larger variability in seasonal MTT_{geo}. The areal coverage of mires was found to be especially important for the contribution of young water in spring ($r=0.96$, $P<0.0001$). The main factor for this was attributed to extensive soil frost in mires, causing considerable overland flow during the snowmelt period. However, this lower groundwater recharge during snowmelt caused mire-dominated catchments to have longer stream runoff MTT_{geo} than comparable forest catchments in winter. Boreal landscapes are sensitive to climate change, and our results suggest that changes in seasonality are likely to cause contrasting responses in different catchments depending on dominating landscape type.

1 Introduction

The age and pathway of water through the terrestrial landscape to stream networks is a widely discussed topic in contemporary hydrology. This interest has emerged because of the significant role residence time, and routing of water through various subsurface environments have on hydrological and biogeochemical processes (McDonnell et al., 2010; Sprenger et al., 2018). This includes fundamental implications for weathering rates (Burns et al., 2003), transport and dispersal of contaminants (Bosson et al., 2013; Kralik, 2015), and accumulation and mobilization of organic carbon and associated solutes (Tiwari et al., 2017). The travel time, from precipitation input to the outflow into streams, provides valuable information about catchment sensitivity to changes in land use and climate, and to the fate of long-range transport of contaminants and nutrients deposited with precipitation (van der Velde et al., 2012). The travel time distribution can vary substantially in time and space, depending on catchment characteristics and hydrological conditions, including, for example, slope, catchment size, soil heterogeneity, and seasonality (Botter et al., 2010; Lin, 2010; Heidbüchel et al., 2012; Hrachowitz et al., 2013). Therefore, estimating travel times for contrasting landscape elements is a challenging task, but when successful, will enhance our ability to understand and predict catchment functioning more adequately.

Stream water consists of a blend of overland flow and groundwater of different ages. The mean travel time (MTT) to streams is calculated as the average age of this mix (McGuire et al., 2006). The baseflow is the part of stream groundwater contribution that is not linked to a specific hydrological episode. Instead, it is the runoff that generally has travelled the furthest and is the oldest (Klaus et al., 2013; Hrachowitz et al., 2016). In contrast, young stream water is typically connected to overland flow or fast and shallow groundwater, which mainly can be seen at times with large rain or snowmelt inputs (Peters et al., 2014; Hrachowitz et al., 2016). Travel times are complex to quantify, especially on intra-annual time scales, as they vary in time and space depending on numerous scale-dependent and independent processes (Botter et al., 2010). A better understanding of the seasonal variability in the fraction of young and old waters can help provide insights into the fundamental role catchment characteristics play in regulating the hydrology and biogeochemistry of streams and rivers.

Stable water isotopes and biogeochemical tracers are common tools applied in field investigations to locate water sources and follow their pathways through the landscape (Maulé and Stein, 1990; Rodhe et al., 1996; Goller et al., 2005; Tetzlaff and Soulsby, 2008). Isotopic tracer dampening can provide an estimate of MTT (Uhlenbrook et al., 2002; McGuire et al., 2005; Peralta-Tapia et al., 2016), and more elaborate time-series analysis can offer quantitative assessments of water age (Harman, 2015; Danesh-Yazdi et al., 2016). Theoretical transfer functions, such as the gamma distribution model, can also be used by relating input and output signals of isotopes, such as precipitation-discharge relationships (McGuire et al., 2005; Hrachowitz et al., 2010; Heidbüchel et al., 2013; Birkel et al., 2016). However, the isotope amplitude signal used to estimate MTT in many transfer functions is lost after approximately four to five years because of effective mixing (Kirchner, 2016), limiting the use of isotopes in catchments with long travel times. The young water fraction, often defined as water younger than two to three months, can, however, still be quantifiable in such catchments (von Freyberg et al., 2018; Lutz et al., 2018; Stockinger et al., 2019). The main advantage of water isotopes is that they are relatively conservative and fractionate primarily because of evaporation. Hence, once in the subsurface environment, the signal is only affected by the mixing of different water sources. In contrast, many biogeochemical tracers react and transform on their route to streams (Lidman et al., 2017; Ledesma et al., 2018). Such transformation and reactions depend on the specific solute and soil environment that water encounters and can therefore give qualitative information about groundwater flow pathways (Wolock et al., 1997; Frisbee et al., 2011; Zimmer et al., 2012). Combined information from conservative and

reactive tracers can hence provide an enhanced understanding of hydrological processes as their concentrations and dynamics can tell complementary stories about the specific pathways water take from the source to the recipient stream (Laudon et al., 2011).

A complementary approach to field experiments is numerical modelling, which can help achieve a more complete system understanding. Lumped hydrological models often describe catchments as single integrated entities. In contrast, distributed numerical models can include spatial heterogeneity in input parameters and therefore have the potential to represent catchment processes more mechanistically. In turn, this can lead to a more process-based understanding of hydrology and biogeochemistry at the catchment-scale (Brirhet and Benaabidate, 2016; Soltani, 2017). Two common methods to calculate travel times using numerical methods includes isotope models and particle tracking (Hrachowitz et al., 2013; Ameli et al., 2016; Kaandorp et al., 2018, Yang et al., 2018). Models, however, need – as far as possible – proper tests against empirical observations to build confidence in their result output. Stream discharge, groundwater levels, and tracer data are examples of such validation data that can provide vital information (McGuire et al., 2007; Hrachowitz et al., 2015; Wang et al., 2017). Collection of such field data is costly and time-consuming. Therefore, data for calibration and validation is often limited, and the minimum length and types in data-sparse catchments is currently a topic of increasing interest (Bjerklie et al., 2003; Jian et al., 2017; Li et al., 2018).

Snow-dominated landscapes have received increasing attention in the last decades due to their importance as water resources (Barnett et al., 2005) and their vulnerability to climate change (Tremblay et al., 2011; Aubin et al., 2018). Landscapes with long-lasting snow cover that often melts rapidly in the spring creates both opportunities and challenges for determining stream water age and pathways. The long, snow-rich winters do not only cause protracted periods of winter baseflow with little or no recharge (Spence et al., 2011; Spence and Phillips, 2015; Lyon et al., 2018), they also cause considerable amounts of water during the often short and intensive snowmelt in the spring. Although attempts to assess travel times generally have provided useful results using gamma distribution functions in snow-dominated catchments, the winter season has proven to be especially challenging suggesting that other methods to assess travel times may be required (Heidbüchel et al., 2012; Peralta-Tapia et al., 2016). The boreal region also consists of numerous patches of lakes and mires, interspersed in a landscape dominated by coniferous forests on different soil types making this task even more challenging. Hence, accounting for the unique circumstances of both baseflow with long travel times and those of the intensive spring snowmelt with potential large overland flow components in heterogeneous landscapes requires models that can handle the complexity and separation of various flow components across scales, soil types and landscape patches.

To overcome previous limitations, this study used particle tracking in the physically-based distributed numerical model, Mike SHE (Graham and Butts, 2005), to enhance our understanding of stream water contribution in boreal landscapes across seasons and landscape configurations. The water movement model in Mike SHE calculates saturated (3D) groundwater flow and unsaturated (1D) flow and is fully integrated with the surface water and evapotranspiration. The water flow model setup and results previously presented by Jutebring Sterte et al. (2018) were used as the study platform for this work. The model has been calibrated and validated to 14 sub-catchment using daily stream-discharge observations and periodical measured groundwater levels in 15 wells throughout the Krycklan catchment in the boreal region of northern Sweden (Laudon et al., 2013; Jutebring Sterte et al., 2018). The model complexity allows for an in-depth investigation of advective travel times by non-reactive particle tracking simulations in a transient flow field.

The main objective of this study was to quantify yearly and seasonal age distributions and calculate MTT of water runoff to streams of the Krycklan sub-catchments to disentangle how these are related to physical landscape characteristics and seasonality. Firstly, the credibility of the model results was tested by comparing calculated travel times for the 14 sub-catchments to ten-year seasonal isotope signatures and base cation concentrations record from the Krycklan network. The usefulness of stream isotopic composition and chemistry record has previously been demonstrated for understanding the connection of hydrological flow pathways and travel times for this site (Laudon et al., 2007; Peralta-Tapia et al., 2015), but with the limitation of studies on only short periods or single catchments. Secondly, the purpose was to go beyond what was previously done by identifying the connection between travel times and different catchment characteristics and test how this varies between variable hydrologically conditions. This was accomplished by capturing contrasting seasons such as the low flow conditions in winter with limited input of new precipitation, high flow in spring when the system is still partly frozen, and summer when evapotranspiration (ET) becomes a significant process. We focused especially on the catchment characteristics that have been suggested to be important factors for regulating stream chemistry of the Krycklan sub-catchments, including the areal coverage of mires, catchment size, soil properties, and seasonal changes in groundwater recharge (Karlsen et al., 2016; Klaminder et al., 2011; Laudon et al., 2007; Peralta-Tapia et al., 2015; Tiwari et al., 2017).

2 Method

2.1 Site Description

The Krycklan study catchment, located in the boreal region at the transition of the temperate/subarctic climate zone of northern Sweden, spans elevations from 114 to 405 m.a.s.l (Fig. 1, Table 1). The characteristic features of this boreal landscape are the dominance of Scots pine (*Pinus sylvestris*) and Norway spruce (*Picea abies*), covering most of the catchment (Laudon et al., 2013). Krycklan has a landscape distinctively formed by the last ice age (Ivarsson and Johnsson, 1988; Lidman et al., 2016). At the higher elevations to the northwest, which are located above the highest postglacial coastline, the till soils can reach up to 15-20 m in thickness. Here, the soil primarily consists of glacial till, and the landscape is intertwined with lakes and peatlands. In this study, we refer to soil as all unconsolidated material above the bedrock. The decreasing hydraulic conductivity with depth is characteristic for glacial tills in northern Sweden (Bishop et al., 2011; Seibert et al., 2009) with conductivities close to $5 \cdot 10^{-5}$ m/s at the ground surface and exponentially decreasing downwards (Nyberg, 1995). At lower elevations, the soils consist of fluvial deposits of primarily sandy and silty sediments. Compared to the soil at higher elevations in the catchment, these deposits can reach thicknesses up to approximately 40 to 50 m and have hydrological conductivity that is more constant with depth.

For more than 30 years, multi-disciplinary biogeochemical and hydrological studies have been conducted in Krycklan (e.g., Laudon and Sponseller, 2018). Streamflow is monitored in 14 nested sub-catchments, called C1 to C20, with the longest continuously monitored time-series starting at the beginning of the 1980s. Connected by a network of streams, the different sub-catchments allow an evaluation of the effects of catchment characteristics on hydrologic transport, including soil type, vegetation, and differences in topography (Table 1).

Table 1: Sub-catchment characteristics. The list includes all 14 monitored sub-catchments in Krycklan, called C1 to C20, including the entire Krycklan catchment, C16. Different branches of the stream network are illustrated in distinct colours in Fig. 1. The table includes the sub-catchment area, average elevation, and average slope. Further descriptions of these characteristics can be found in Karlsen et al. (2016). The table also includes soil proportion based on the soil map (1:100,000) from the Swedish Geological Survey (2014).

	Catchment size (km^2)	Average elevation (m.a.s.l.)	Slope (°)	Till (%)	Mire (%)	Sandy sediments (%)	Silty sediments (%)	Lake (%)
C1	0.48	279	4.87	91	0	0	0	0.0
C2	0.12	273	4.75	79	0	0	0	0.0
C4	0.18	287	4.24	29	42	0	0	0.0
C5	0.65	292	2.91	47	46	0	0	6.4
C6	1.10	283	4.53	51	29	0	0	3.8
C7	0.47	275	4.98	68	16	0	0	0.0
C9	2.88	251	4.25	64	14	7	4	1.5
C10	3.36	296	5.11	64	28	1	0	0.0
C12	5.44	277	4.90	70	18	6	0	0.0
C13	7.00	251	4.52	60	10	9	9	0.7
C14	14.10	228	6.35	46	6	24	15	0.7
C15	19.13	277	6.38	64	15	8	2	2.4
C16	67.90	239	6.35	51	9	21	10	1.0
C20	1.45	214	5.96	55	9	0	28	0.0

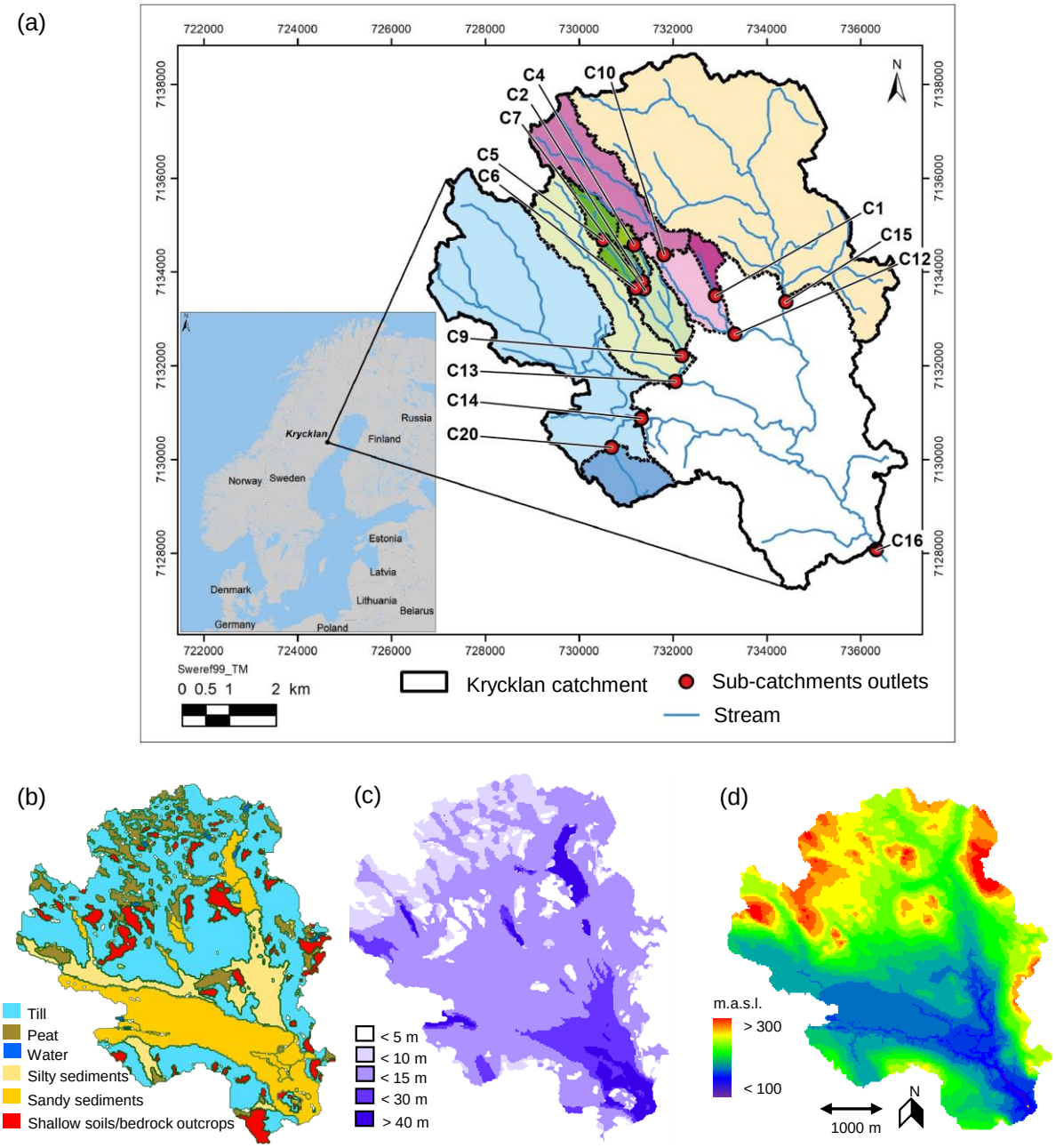

Figure 1: The Krycklan catchment. (a) Location of sub-catchment and their outlets. The areas are color-coded based on their stream network connections, e.g., all sub-catchments of one colour connect before reaching the white area. For further details of the catchment characteristics, see Table 1. (b) The soil map used in the Mike SHE flow model and is based on the soil map (1:100,000) from the Swedish Geological Survey (2014), combined with field investigations. (c) Depth to bedrock from the Swedish Geological Survey (2014) is shown in meters below the ground surface. (d) Catchment topography, shown as meters above sea level (m.a.s.l.).

2.2 Linking seasonal base cation concentration and isotopic signature to stream water age

This study was focused on three seasons in Krycklan, winter, spring, and summer. We defined the winter to occur from late November to late March because it is characterized by an extensive and permanent snow cover with little groundwater recharge. We assumed that the winter stream composition reflects the chemistry of deeper groundwater (Fig. 2). Similarly, we defined spring by the rapid transition in hydrology and biogeochemistry in April-May. During snowmelt, ca 50 % of the annual precipitation

leaves the system in a short period of time, diluting baseflow with new input of water. Finally, we defined the summer season as the period between July and September when the hydrology is characterised by rain, high ET and relatively little runoff. June and October were excluded because, hydrologically, they are transition months between the three distinct seasons. This is because snowmelt can still influence runoff in June, and winter conditions (snowfall, soil frost, etc.) can sometimes begin to establish in October.

In this study, stable water isotopes ($\delta^{18}O$) were used to track pathways of precipitation inputs to stream networks (see Appendix for the $\delta^{18}O$ definition). Ten years of $\delta^{18}O$ results for 13 of the 14 sub-catchments were used. Some of the sub-catchments are affected by evaporation from lake surfaces that result in isotopic fractionation that, consequently, affected the signal (Leach and Laudon, 2019). This fractionation was corrected for the percentage of lakes in each sub-catchment (Table 2), using the same principle as Peralta-Tapia et al. (2015) but adjusted to newly acquired $\delta^{18}O$ observations.

The comparison of the modelling results to observations of $\delta^{18}O$ was based on a conceptual model of the seasonal variability and differences between precipitation and runoff (Fig. 2a). Because there is no groundwater recharge during winter, the stream isotopic signature originates from groundwater only (Laudon et al., 2007). Hence, we assumed that $\delta^{18}O$ during winter baseflow should be statistically related to the average age of the groundwater (up until the point where full mixing is reached). The closer the signature is to the long-term precipitation average (which is equal to the deep groundwater measurements in Krycklan (Laudon et al., 2007)), the more well-mixed and, consequently, the older the average groundwater has become. In spring, previous studies have shown that the young water fraction can be distinguished by comparing the change in the isotopic signature to the preceding winter because the snow is much lighter (depleted in ^{18}O) (Laudon et al., 2007; Tetzlaff et al., 2015). We refer to the difference between the average winter and average spring signature as the $\Delta\delta^{18}O_{spring}$, which we assumed to be negatively correlated to the young water fraction (Fig. 2a). Similarly, we refer to the difference between the average winter and average summer signature as $\Delta\delta^{18}O_{summer}$, which similarly should be related to the young water fraction during the summer. However, in summer, precipitation is heavier (more enriched in ^{18}O) compared to winter, which hence should give the young water a heavier signal. Therefore, we assumed a positive relationship between the young water fraction and the $\Delta\delta^{18}O_{summer}$ (Fig. 2a).

Another indicator of stream water age we used was the sum of base cations (BC) concentration (Fig. 2b) (Abbott et al., 2016). Previous attempts to follow the chemical development of groundwater in the Krycklan catchment and other streams have shown that the BC concentration increases along the groundwater flow pathway (Klaminder et al., 2011). Therefore, a correlation between the stream concentration of BCs on the one hand and modelled soil contact time on the other were assumed in this study. The BCs are mainly derived from the weathering of local soils in the Krycklan catchment, with only a minor contribution from atmospheric deposition (Lidman et al., 2014). Our assumption is further based on modelling studies of weathering rates in a soil transect in the Krycklan catchment, which indicates that there is kinetic control of the release of BCs in the soils (Erlandsson et al., 2016). Since all BCs behave relatively conservatively in these environments (Ledesma et al., 2013; Lidman et al., 2014), we used their combined concentration as a proxy for soil contact time. However, the assumption is only valid when the water is in contact with mineral soils, not with peat in mires, which are abundant in some of the investigated sub-catchments. There are no minerals present in the peat and, therefore, the BC concentration cannot be expected to increase during the time the water spends there. Therefore, the BC concentrations were adjusted for the influence of mire, using the sub-catchment mire proportion as a scaling factor to allow a fair comparison to water soil contact time (Lidman et al., 2014) (Table 2).

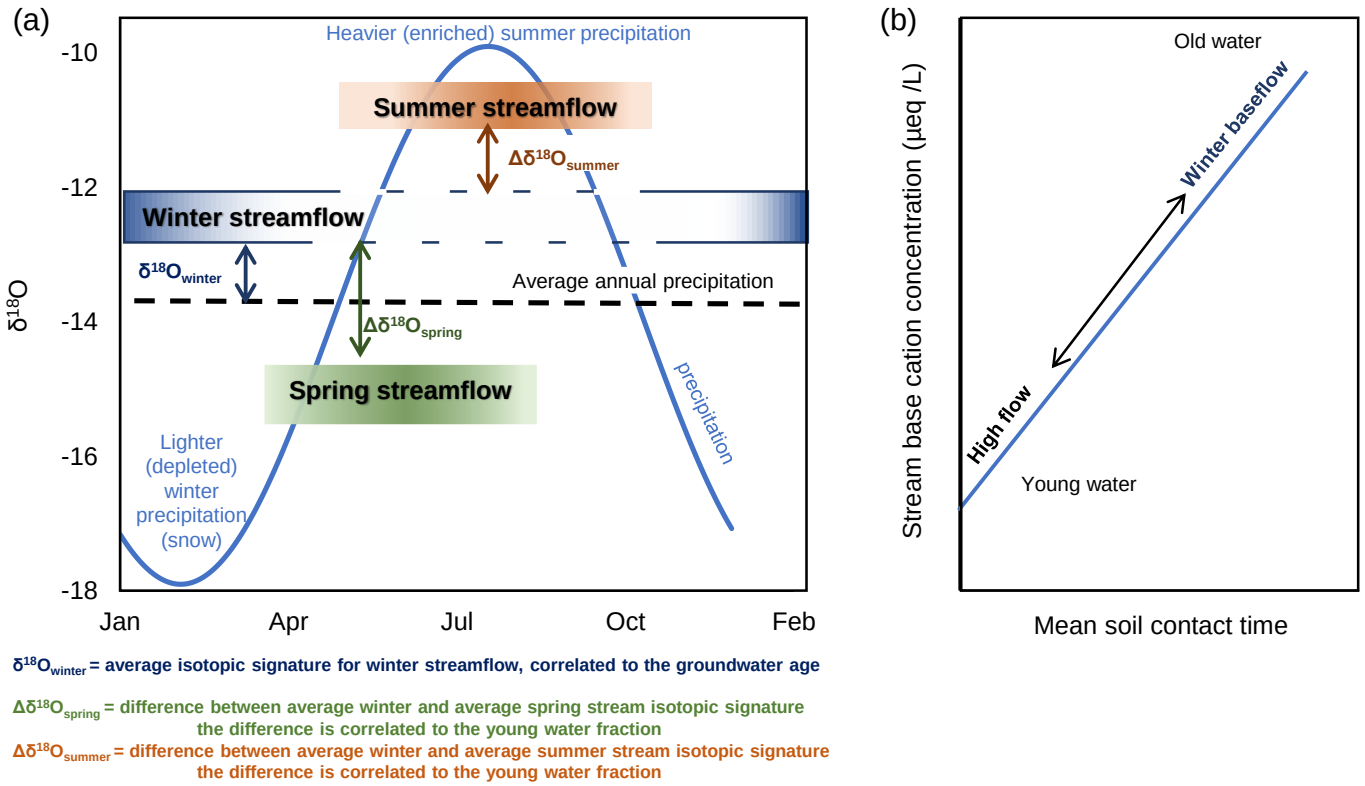

Figure 2: Conceptual figure of stream water travel time vs. stream isotopic signature (a) and stream base cation concentration (b). (a) The connection between $\delta^{18}O$ and stream water travel time, where the sine curve shows the annual variations of $\delta^{18}O$ in precipitation, and approximate seasonal winter, spring, and summer stream composition are marked. In winter, the travel times are related to the deviation in the isotopic signature between the winter baseflow and the long-term precipitation. In spring, the fraction of young water is correlated to the difference between the spring stream signature and the winter baseflow. In summer, the fraction of young water is correlated to the difference between the stream signature and winter baseflow. (b) The connection between base cation (BC) concentration and soil contact time. The longer water spent in the mineral soil, the higher the stream concentrations of BCs due to soil weathering.

All stream chemistry data comes from the online open Krycklan database at www.slu.se/Krycklan (Table 2). The isotopic signatures contain approximately ten years of field observations (2008 to mid-2018), approximately 25 samples per year for each site. Parts of the dataset have been published by Peralta-Tapia et al. (2016), where sampling and analyses are described in detail. It has since been expanded using the same methodology. We used the average winter isotope signatures from these years as a representation of baseflow. These averages were also compared to the volume-weighted average of the long-term precipitation, calculated using 1160 precipitation measurements of $\delta^{18}O$ between 2007 and 2016. The precipitation was measured throughout the year, both as rain and as snow. The long-term precipitation average is -13.5 ‰, which is equal to observations of the isotopic signature at the deep groundwater wells of Krycklan (10 m depth). The BC data collection methodology is reported in Ledesma et al. (2013).

Table 2: Seasonal stream chemistry.

	$\delta^{18}O$[a]						Base cations (BC)[b]					
	Winter		Spring		Summer		Winter concentration		Spring concentration		Summer concentration	
	‰	SD/SEM[c]	$\Delta\delta^{18}O$	SD/SEM	$\Delta\delta^{18}O$	SD/SEM	µeq/L	SD/SEM	µeq/L	SD/SEM	µeq/L	SD/SEM
C1	-12.9	0.28/0.05	-0.53	0.60/0.18	0.10	0.38/0.19	283	39/7	211	36/5	285	31/4
C2	-12.9	0.46/0.07	-0.68	0.52/0.16	0.15	0.45/0.16	288	104/21	174	41/6	267	58/9
C4	-13.1	0.36/0.06	-1.08	0.66/0.20	0.82	0.48/0.21	295	77/17	107	33/5	306	77/12
C5	-13.0	0.47/0.08	-1.80	0.66/0.20	0.72	0.65/0.21	273	27/6	172	49/9	231	34/5
C6	-13.1	0.35/0.06	-1.27	0.55/0.16	0.52	0.47/0.17	364	80/16	230	133/19	322	120/16
C7	-13.0	0.22/0.04	-0.73	0.56/0.17	0.42	0.37/0.18	290	43/9	177	59/9	270	38/5
C9	-13.1	0.29/0.05	-0.98	0.46/0.14	0.57	0.44/0.15	385	61/12	219	87/13	327	61/8
C10	-13.3	0.28/0.05	-0.80	0.61/0.18	0.53	0.39/0.19	348	58/12	200	104/16	332	72/10
C12	-13.1	0.30/0.05	-0.88	0.48/0.15	0.36	0.43/0.16	349	48/10	187	40/6	316	45/6
C13	-13.1	0.26/0.05	-0.83	0.55/0.16	0.60	0.48/0.17	379	57/12	203	37/5	309	43/6
C14	-13.4	0.23/0.04	-0.70	0.55/0.17	0.48	0.45/0.18	388	46/10	264	85/12	376	74/10
C15	-13.4	0.40/0.07	-0.73	0.69/0.21	0.63	0.44/0.22	373	44/9	233	41/6	349	45/6
C16	-13.4	0.44/0.08	-0.56	0.64/0.64	0.46	0.33/0.20	511	56/11	251	53/8	441	76/10
C20	-	-	-	-	-	-	582	80/17	348	48/7	526	60/8
Long term precipitation average												
	-13.5 ‰ [d]						80 µeq L^{-1} [d]					

[a] $\delta^{18}O$ Signature (2008-2018), data have been adjusted according to the lake proportion
[b] Base cation concentration (2008-2016), data has been adjusted according to the mire proportion
[c] SD = standard deviation, SEM = standard error of the mean
[d] Measured precipitation average for isotopes (2007-2016) and measured BC concentration (the year 1997 to 2018)

2.3 Water flow model setup

We applied the Mike SHE/Mike-11 hydrological modelling tools to quantify travel times in a pre-calculated 3D transient flow field. The simulated terrestrial hydrological system for the Krycklan catchment includes: the saturated and unsaturated flow, ET, snowmelt, overland flow, and streamflow processes. The fully distributed 3D modelling tool use topography, soil properties, and time-varying climate inputs to calculate the water fluxes throughout a catchment (Rahim et al., 2012; Sishodia et al., 2017; Wang et al., 2012; Wijesekara et al., 2014). The ET processes include canopy interception, open surface evaporation, root uptake, sublimation, and soil evaporation from the unsaturated zone based on a methodology developed by Kristensen and Jensen (1975). Flow in the saturated zone (SZ) is calculated in 3D by the Darcy equation. The flow in the unsaturated zone (UZ) is calculated in vertical 1D using the Richards equation, and overland flow (OL) is calculated using a horizontal 2D diffusive wave approximation in the Saint-Venant equations (Fig. 3). Streams are modelled in 1D using a high-order dynamic wave formulation of the Saint-Venant equations. The river model (Mike 11) is not restricted to the grid size of Mike SHE and allows for a more precise calculation of stream water levels and flow rates. The different model compartments OL, UZ, SZ, and rivers are fully integrated, and water fluxes between and within the compartments are calculated in each time step of the simulation. More in-depth documentation and manuals of Mike SHE and Mike 11 is provided by Mike powered by DHI (www.mikepoweredbydhi.com).

For the Krycklan model, the horizontal grid was set to 50*50 m. Vertically, the model is divided into ten calculation layers (CL) and extends to a depth of 100 m below ground. The CLs of the SZ vary with depth and are thinner closer to the soil surface; the first CLs extend to 2.5, 3, 4, and 5 meters below the ground surface, with the soil properties and depth extension following the stratigraphy (Table 3). The ET and UZ processes are only fully active in the uppermost SZ-CL, and here the ET and UZ are

calculated at a finer resolution, leading to a detailed calculation of the groundwater table level. If the groundwater table falls below the first SZ-CL, a more simplistic method, not taking capillary rise and all ET-processes into account, was applied. The depth of the first SZ-CL was set to 2.5 m and was calibrated using the influence of the CL thickness on groundwater table level, UZ, and ET dynamics.

The thickness of the first SZ-CL in the Krycklan model results in all soils shallower than 2.5 meters being averaged into one soil type. In Mike SHE, horizontal hydraulic conductivity (Kh) is averaged using the thickness of each soil layer. Vertical flows are more dependent on the lowest vertical hydraulic conductivity (Kv). Therefore, the harmonic weighted mean value is used to calculate the new Kv instead (Table 3). In the Krycklan model, and several previous studies (Bosson et al. 2012, 2013, Johansson et al. 2015 and Jutebring et al. 2018), a drain function was used to account for higher hydraulic conductivity in the uppermost part of the first CL. In the Krycklan model, the function was activated whenever the groundwater reached 0.5 m below the ground surface, above which higher K-values have been observed (Table 3) (Bishop et al., 2011; Nyberg, 1995; Seibert et al., 2009). The model also accounted for soil freezing processes, which in Krycklan has been shown to have a strong influence on the water turnover in mires (Laudon et al., 2011). Based on a methodology presented in Johansson et al. (2015), soil freeze and thawing processes were described using time-varying K and infiltration capacity.

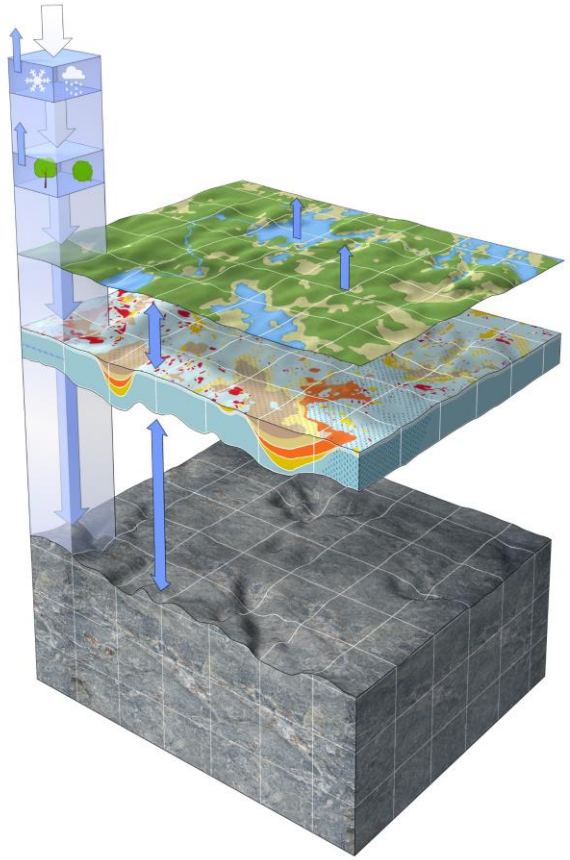

Figure 3: Schematic Mike SHE model set up. Precipitation falls on the ground as rain or snow. Evapotranspiration (ET) processes include canopy interception, open surface evaporation, root uptake, and soil evaporation from the unsaturated zone (UZ). The overland flow (OL), saturated zone (SZ), and UZ interact depending on the saturation level. The SZ is divided into ten calculation layers (CL), while the UZ has a much finer description. Streamflow is modelled through Mike 11 and is not restricted to the Mike SHE resolution. The figure is used on the courtesy of SKB. Figure illustrator: LAJ.

The Krycklan flow model was able to reproduce observed stream accumulated discharge, groundwater levels, and timing of precipitation events (Jutebring Sterte et al., 2018). These include daily discharge observations (14 streams) and weekly to monthly observed groundwater levels (15 wells) for 2009-2014. The accumulated error in stream discharge was on average 11%, and highest for sub-catchments with few observation points (<25%). For this study, a few changes were made to the Krycklan model (Jutebring Sterte et al., 2018). Most importantly, new field data from the Krycklan database gave a more precise location of the observation station at C5 (red circle in Fig. 1). The Kh of silt was also increased from $1*10^{-8}$ m/s to $1*10^{-7}$ m/s due to new soil property samples, which gave a slightly better flow representation of the sites affected silty sediments. However, the corrections and additions did not influence the model results in any substantial way. The improvements were small but were made to better represent the site according to all available data.

Table 3: Flow model setup. Flow model setup from the calibrated and validated Mike SHE model presented in Jutebring Sterte et al. (2018). The "soil type surface" corresponds to the soil type shown in Fig. 1b. A drain constant was used to account for coarser material of the upper half meter of the soil.

Soil type surface	Depth below ground (m)[a]	Soil type	Horizontal hydraulic conductivity (m/s)	Vertical hydraulic conductivity (m/s)
Till	2.5	Till	$2*10^{-5}$	$2*10^{-6}$
	To bedrock	Fine till	$1*10^{-6}$	$1*10^{-7}$
	Bedrock		$1*10^{-9}$	$1*10^{-9}$
Peat	5	Peat	$1*10^{-5}$	$5*10^{-5}$
	7	Clay	$1*10^{-9}$	$1*10^{-9}$
	To bedrock	Fine till	$1*10^{-6}$	$1*10^{-7}$
	Bedrock		$1*10^{-9}$	$1*10^{-9}$
Silty sediments	3	Silt/clay	$1*10^{-7}$	$1*10^{-7}$
	To bedrock	Fine till	$1*10^{-6}$	$1*10^{-7}$
	Bedrock		$1*10^{-9}$	$1*10^{-9}$
Sandy Sediments	4	Silt/Sand	$2*10^{-5}$	$2*10^{-5}$
	0.9*max depth	Sand	$3*10^{-4}$	$3*10^{-5}$
	To bedrock	Gravel	$1*10^{-4}$	$1*10^{-4}$
	Bedrock		$1*10^{-9}$	$1*10^{-9}$
Drain constant				
Peat	$1*10^{-6}$			
Till	$4*10^{-7}$			
Silty sediments	$1*10^{-7}$			

[a] The table shows the depth to which the same description extends to. For example, the first description of Peat extends down to five meters, while the first calculation layer is 2.5 meters.

2.4 Establishing travel times - Particle tracking

Particle tracking in Mike SHE enables investigations of groundwater travel time from recharge into the SZ until reaching the streams, as described in detail in Bosson et al. (2010, 2013). The model calculates the location and age of separate particles added with infiltrating water along their flow lines. The particles move by advection governed by the pre-calculated groundwater flow field from the Mike SHE model (Jutebring et al., 2018). This method allows for long-term transport calculations where particle tracking can be run for several annual cycles based on the same transient or steady-state flow field. The advection-dispersion equation governs the transportation of particles for a porous medium. The Darcy velocity is divided by the porosity to calculate the groundwater velocity. Therefore, the only complementary input data needed to run the particle was porosity values (Table 4).

Particle tracking was used to assess groundwater travel times from groundwater recharge to stream runoff for each sub-catchment. The model was run for 1000 years to capture the travel times of all discharging groundwater for each sub-catchment. One year of simulated flow results from Jutebring Sterte et al. (2018) was cycled 1000 times to extend the particle tracking simulation. The year 2010 was selected, as the water balance was close to the long-term annual averages observed for the Krycklan catchment. All particles were released at the top of the transient groundwater table the first year. Numerical constraints restricted the number of particles released to 0.5 particles/10 mm modelled groundwater recharge, which corresponds to a total of approximately 0.6 million particles. This number of particles was assumed to be enough to capture the timing of recharge patterns (Fig. 4).

Table 4: Porosity values for different soil types used in the Mike SHE model.

Soil type	Porosity (-)
Gravel [a]	0.32
Sand [b]	0.35
Silt [c]	0.45
Clay [b]	*0.55
Silt-clay [d]	0.50
Till [b]	0.30
Peat [b]	0.50
Bedrock [b]	0.0001
Bedrock fractures/deformation zones [b]	0.001

[a] Average of Morris and Johnson. (1967). [b]Joyce et al. (2010). [c] Average value between sand and clay. [d] Average value between silt and clay

2.5 Analysis of modelled travel times, relationship to stream chemistry and landscape characteristics

The time it took for particles to reach a stream or lake via groundwater (hereafter called 'travel time') was calculated for each sub-catchment both annually and for each season. The calculated travel time distributions were analysed using four statistical measurement tools, the arithmetic mean, the geometric mean, median, and the standard deviation (SD). The arithmetic mean, the geometric mean and the median are common choices to describe the central tendency of a distribution (Destouni et al., 2001; Kaandorp et al., 2018; Massoudieh et al., 2012, 2017; Unlu et al., 2004), which all have their strengths and weaknesses. If the distribution is significantly skewed, the SD is larger than half of the average (Taagepera, 2008). In the case of the observed $\delta^{18}O$ and BC concentrations (Table 2), the SD is much smaller than half of the average. Therefore, the arithmetic mean was used to describe the central tendency of the data set. However, if the travel time distribution becomes skewed, the arithmetic mean becomes highly sensitive to the tail of the distribution and produces considerable uncertainty. In these cases, the median and the geometric mean are often better as a measure of the central tendency, of mean travel time (MTT), than the average. However, to compare the MTT of discharged water of different streams, we still wanted the metric to account for the length of the tail. Therefore, we used the geometric mean because the median only states the middle value of a distribution regardless of the tail length (Taagepera, 2008; Unlu et al., 2004; Zhang et al., 1996). However, we provide all metrics, including the arithmetic mean, the geometric mean, median, and SD in the Appendix, Table A1.

The MTT was compared to stream chemistry, which is a mix of both groundwater and surface water. In winter, all streamflow contributions originate from groundwater. Here the results from the particle tracking reflect the actual travel time to the streams. However, in summer and especially in spring, some water will reach the streams via overland flow (OL), which has not spent any time in the ground. Since the particle tracking does not take surface flow into account, OL was accounted for by reducing the MTT

by using the OL fraction as a scaling factor. The young water, young water fraction was also used as an evaluation criterion. Like previous studies (Kirchner., 2016; von Freyberg et al., 2018; Lutz et al., 2018; Stockinger et al., 2019), we assumed young water fraction to be the sum of all water less than three month old. In our case, this includes all water reaching streams as overland flow and as young groundwater (<three months). The modelled MTT and young water fraction were also used to identify the main factors determining the age of stream water. The catchment characteristics tested included important terrain factors such as catchment size, slope, and main soil types (Table 1).

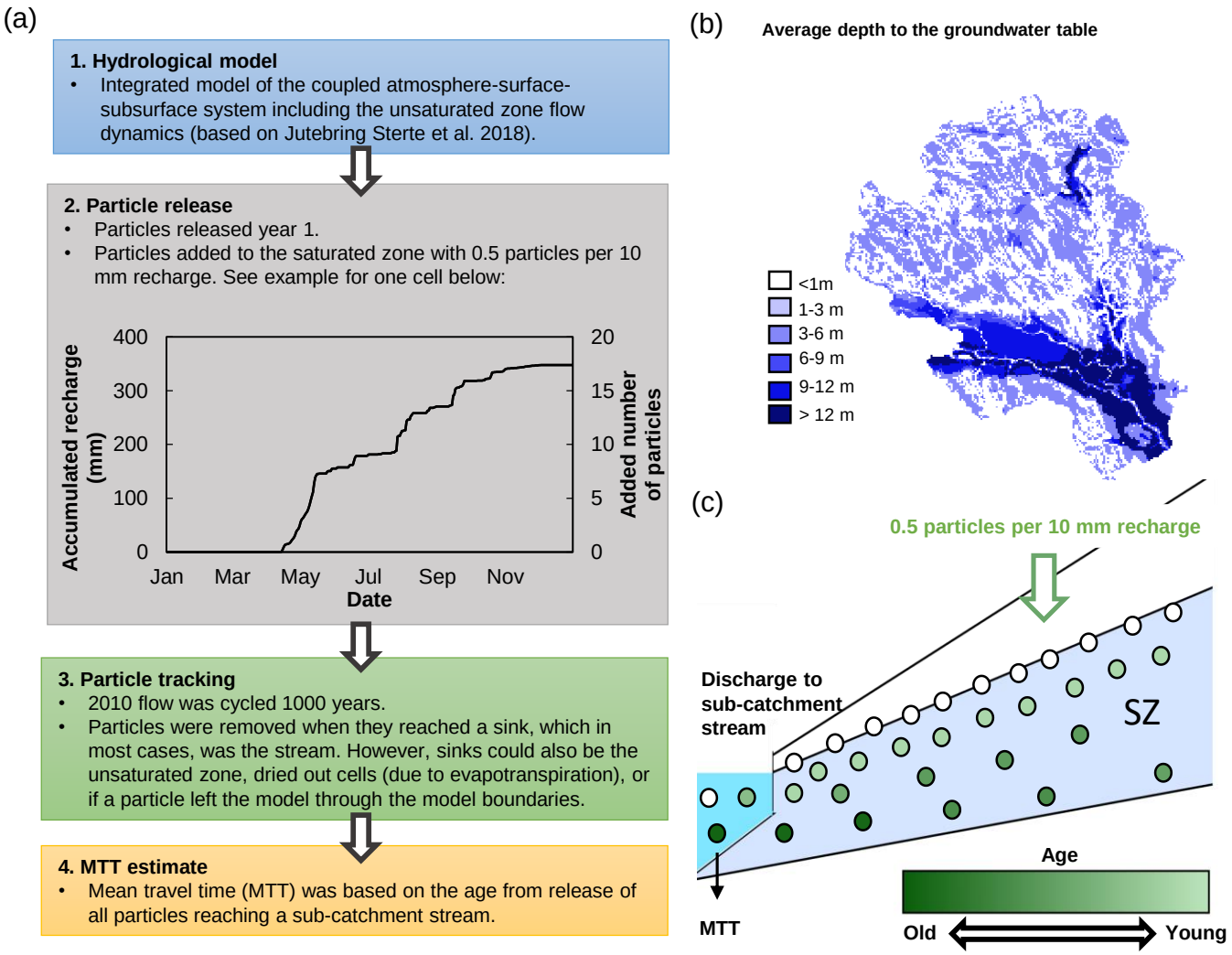

Figure 4: Particle model setup. (a) Steps of particle tracking (b) Average depth to the groundwater table. The main part of the model area has a calculated depth to the groundwater table between 0-3 m and varied daily. (c) Schematic illustration of particle tracking set up. Particles were added to groundwater recharge at the transient groundwater table. The age of these particles was zero at the time of recharge, then followed the groundwater flow resulting in increasing age until reaching a stream or lake.

3. Result

3.1 Travel time results

The particle tracking results were used to establish travel time distributions and MTT of stream water runoff of the 14 sub-catchments in Krycklan. Since the travel time distributions were significantly skewed, we assumed that the geometric mean of the travel time distributions provided the best representation of MTT (Table 5, Fig. 5). However, all metrics are stated in the Appendix, Table A1. The annual MTT_{geo} for all sub-catchments ranged from 0.8 to 3.1 years (Table 5). Most groundwater discharging to a stream had a travel time of less than one year (34% to 54%). The longest stream MTTs were connected to silt dominated catchments such as C16 and C20. We used some sub-catchments for result representation, but all results are provided in Table 5 and Appendix A1. The displayed sub-catchments were: C2 (small till and forest dominated catchment), C4 (small mire dominated catchment), C20 (small silt dominated catchment), and C16 (the full-scale Krycklan catchment).

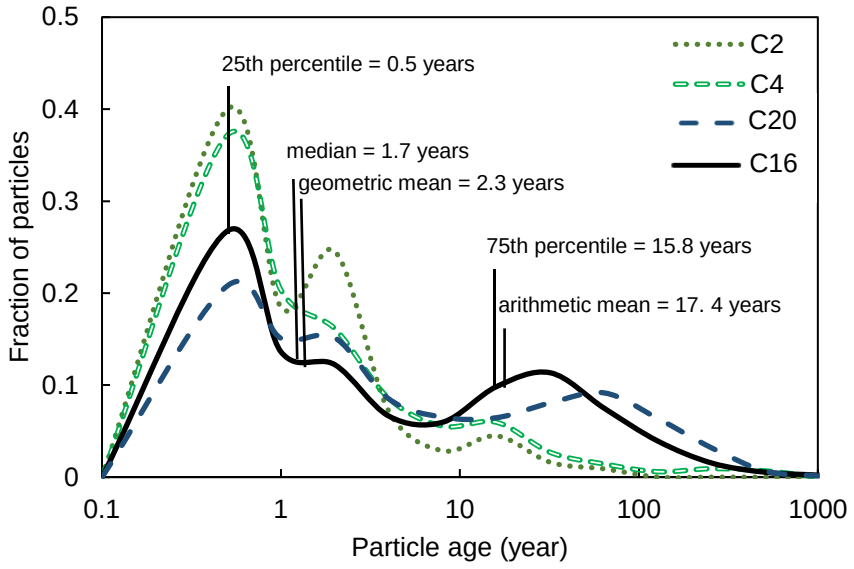

Figure 5: Examples of particle tracking results. The figure shows the age of particles reaching sub-catchment outlets. The solid line showcases the statistics for C16, including the 25th percentile, the median, the geometric mean, the arithmetic mean, and the 75th percentile (Appendix, A1). Moreover, the figure shows three other example distributions, including C2 (small forest and till dominated catchment), C4 (small mire dominated catchment), C20 (small silt dominated catchment).

On an annual basis, a fraction of water reached the streams as overland flow. A major part of the overland flow occurred during the snowmelt in spring, especially in sub-catchments with mires such as C4 (Fig. 6). Both the fraction of young water reaching the streams and the MTT_{geo} displayed strong seasonal trends. The longest seasonal MTT_{geo}, 1.2-7.7 years, and the smallest young water fraction were found during the winter season. In winter, the fraction of older water successively increased until the spring snowmelt began in early April. Conversely, the smallest fraction of old discharging water and short MTT_{geo}, 0.5-1.9 years, were connected to events of larger groundwater recharge, such as the spring snowmelt and heavy summer rains.

In spring, mire sub-catchments had the shortest MTT_{geo}. However, as exemplified by the similar-sized C2 and C4 sub-catchments, groundwater was not renewed to the same extent in mire dominated systems due to a larger fraction surface runoff (Fig. 6). Mire dominated sub-catchments (like C4) displayed stronger seasonal variations in MTT_{geo}, with shorter MTT_{geo} than till dominated sub-catchments (like C2) in spring and longer MTT_{geo} than C2 in winter (Table 5). In C4, the MTT_{geo} reduced from 1.5 to 0.7 years

from winter to spring, while the corresponding change in C2 was 1.2 to 0.7 years. The seasonality of MTT_{geo} was even more pronounced for catchments with a larger areal coverage of mires combined with a larger areal coverage of silt. For example, C20 had an MTT_{geo} that reduced from 7.7 years to 1.9 years from winter to spring, compared (Table 5).

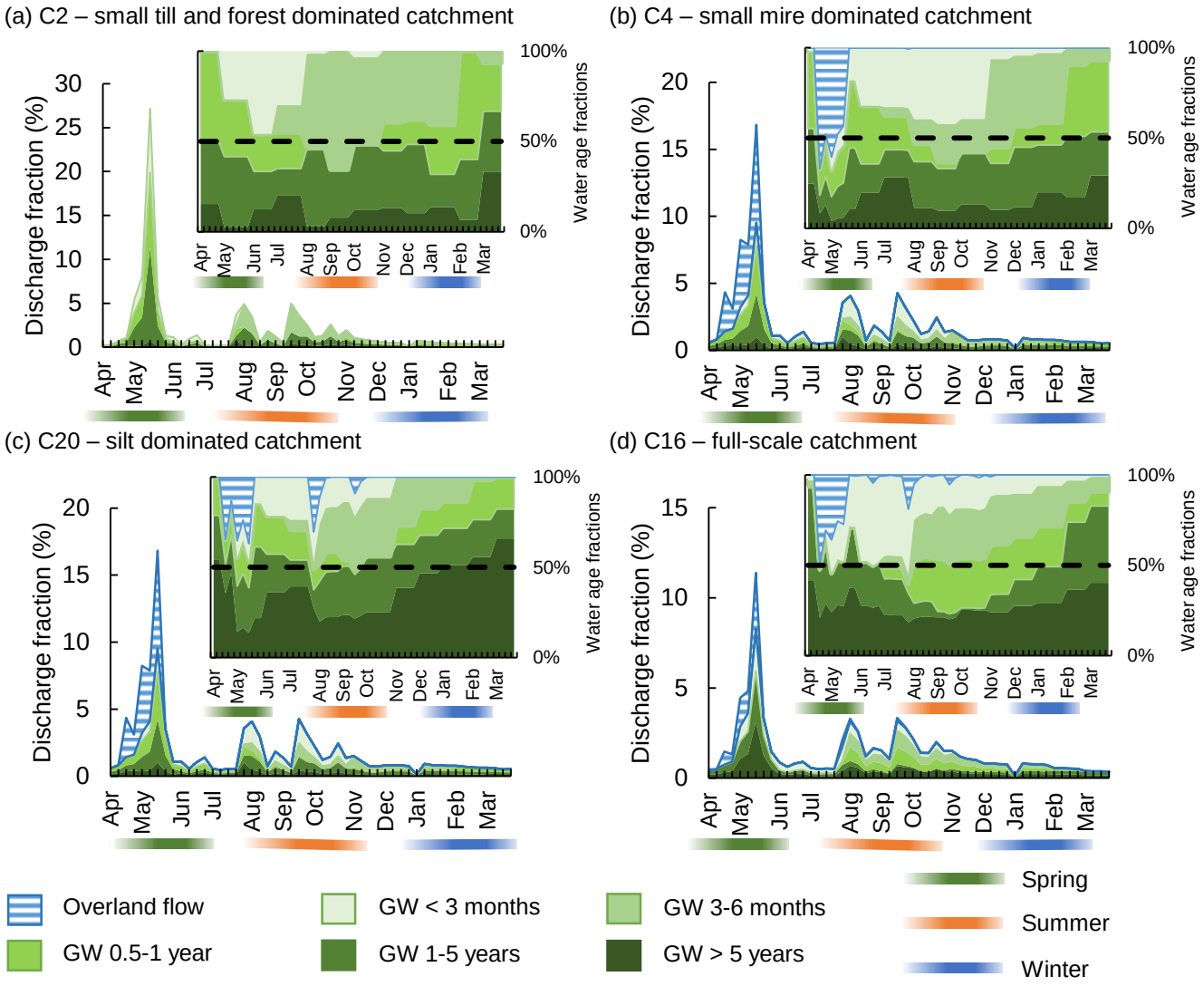

Figure 6: Seasonal fraction of discharge to streams. The figure shows the proportion of annual stream discharge arriving as groundwater and overland flow. Four sub-catchments are exemplified, including (a) the small till and forest dominated C2, (b) the small mire dominated C4, (c) the silt dominated C20, and (d) the full-scale Krycklan catchment C16 with mixed mires and forests (extended version in Appendix Fig. A1). The figure showcases the water age fraction discharging to the streams. The fractions are both shown as part of the total annual discharge as well as the water composition. The bands below the months highlight the three investigated seasons, spring, summer, and winter.

Table 5: Annual and seasonal (winter, spring, and summer) travel times
The geometric mean of the travel time distribution (MTT_{geo}) is adjusted for the overland flow. The young water fraction (YWF) includes overland flow and groundwater that is less than three months (%). An extended version of the results, including arithmetic mean, median, and SD, is included in the Appendix, Table A1.

	Annual		Season - Winter		Season - Spring		Season - Summer	
	MTT_{geo}	YWF	MTT_{geo}	YWF	MTT_{geo}	YWF	MTT_{geo}	YWF
unit	year	%	year	%	year	%	year	%
C1	1.3	20	3.0	6	1.0	25	0.9	19
C2	0.8	16	1.2	0	0.7	26	0.7	6
C4	0.8	40	1.5	2	0.7	53	0.7	39
C5	0.8	49	2.9	1	0.5	66	0.8	38
C6	0.9	42	2.8	2	0.6	58	0.8	34
C7	1.1	28	2.2	4	0.9	37	0.9	27
C9	1.4	28	3.4	3	1.0	41	1.1	24
C10	1.1	33	2.5	3	0.8	47	0.9	31
C12	1.3	28	2.8	5	0.9	39	1.1	26
C13	1.4	26	3.3	3	1.0	37	1.2	23
C14	2.4	20	5.6	2	1.6	32	1.6	21
C15	1.5	28	3.8	4	0.9	41	1.1	27
C16	2.3	23	5.3	4	1.4	35	1.6	23
C20	2.7	23	7.7	0	1.9	36	1.5	24

3.2 Testing model results to stream isotopic composition and chemistry

In addition to investigating the annual MTT_{geo}, three distinct seasons were evaluated regarding the stream chemistry: winter, spring, and summer. The isotopic composition was available for 13 out of 14 sub-catchments (C20 excluded because of short time-series), while the base cation (BC) data was available for all sites. In winter, the modelled MTT_{geo} was correlated to isotopic composition ($r=-0.80$, $P<0.01$), with older stream water being closer to the long-term precipitation average (Fig. 7a). Some of the larger sub-catchments had an isotopic signature close to the precipitation average, suggesting almost complete mixing (e.g., C16). The negative correlation between the $\Delta\delta^{18}O_{spring}$ and the young water fraction was also significant ($r=-0.90$, $P<0.0001$, Fig. 7c), following our conceptual model (Fig. 2a). The same was also true for the summer season, but with the opposite sign of the slope since the summer precipitation was heavier compared to the baseflow. The positive correlation was weaker than during the spring season but still significant ($r=0.80$, $P<0.001$, Fig. 7e). The MTT_{geo} had a significant correlation to the BC concentration during all seasons (Fig. 7 b, d, and e), again agreeing with our conceptual model (Fig. 2b). The correlation between the BC concentration and MTT_{geo} was strongest in winter ($r=0.88$ $P<0.0001$) and weakest in summer ($r=0.79$, $P<0.001$). The sub-catchments with the oldest age and highest BC concentration included the sub-catchments with larger areal coverage of silt, for example, C16 and C20. The youngest ages and lowest BC concentrations were connected to smaller sub-catchments, such as C2 and C4.

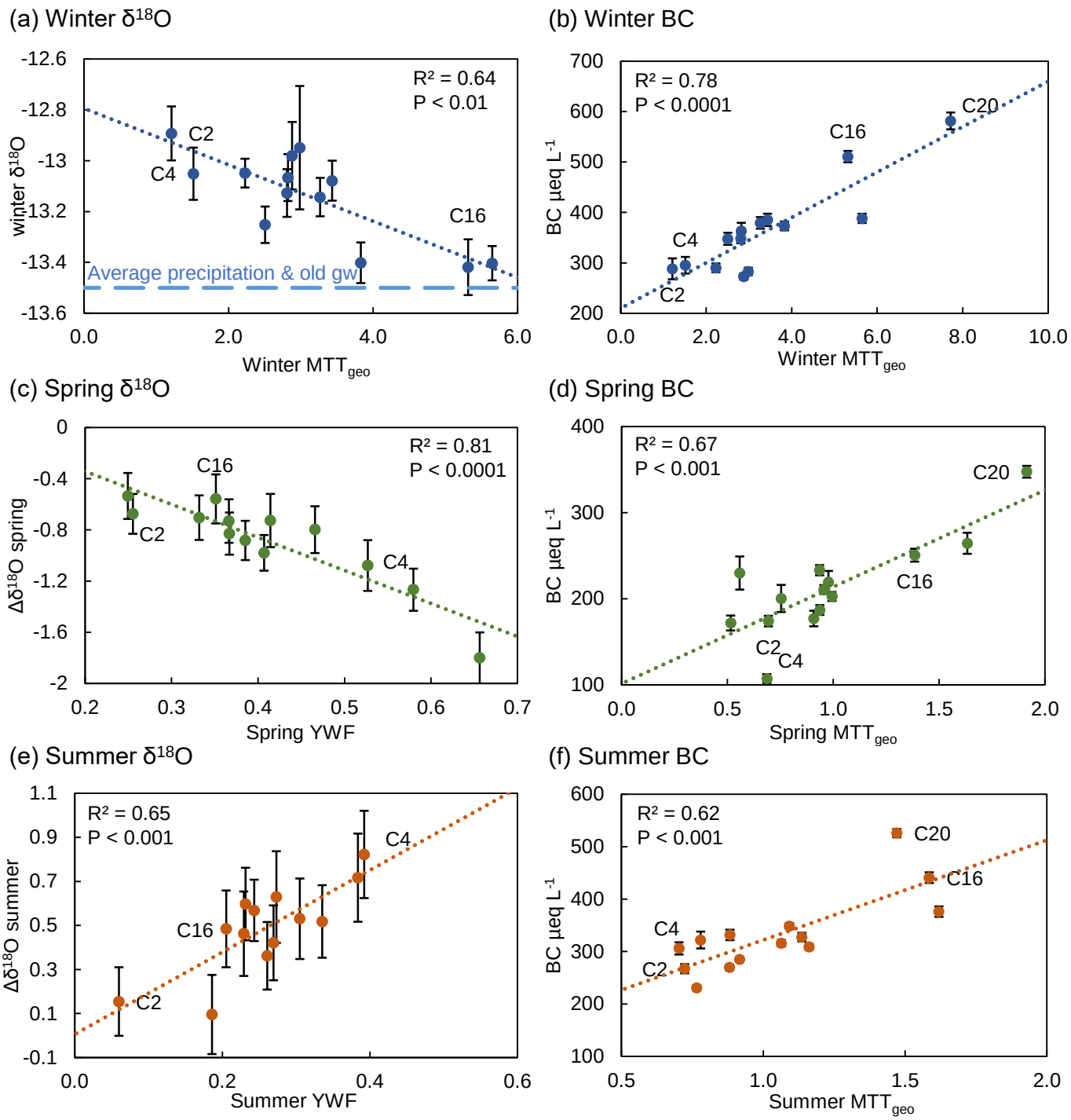

Figure 7: Results of seasonal young water fraction (YWF) and MTT_{geo} compared to stream isotopic composition and base cation concentration. Note that $\delta^{18}O$ results are for 13 sites, while the BC record comprises all 14. The sub-plots (a) to (f) show the $\delta^{18}O$ (winter) or $\Delta\delta^{18}O_{spring/summer}$ and BC concentrations as a function of the MTT_{geo} in winter, spring, and summer, respectively. The standard error of the mean (SEM) shown as whiskers denotes variations in field observations.

3.3 Model results compared to catchment characteristics

The main catchment characteristics correlated to MTT_{geo} and young water fraction were catchment size, the areal coverage of low conductive silty sediments, and the areal coverage of mires. The strongest positive correlation was found between the young water fraction and the areal coverage of mires ($r=0.96$, $P<0.0001$). There was also a strong positive correlation between MTT_{geo} and the

areal coverage of silt (r=0.90, P<0.0001) (Fig. 8). A positive correlation between catchment size and MTT_{geo} was also found, albeit weak due to one catchment, C20, yet significant (r=0.63, P<0.05) (Fig. 8). However, the catchment size was also correlated to the areal coverage of silt, which may be the underlying reason for this correlation (Table 6) as C20 is the only relatively small monitored sub-catchment located in the area with sorted sediments. The annual and seasonal patterns were similar (Table 6). However, the positive correlation between mires and the young water fraction was lost in winter due to a lack of new precipitation input into the system. A weak negative correlation between MTT_{geo} and the young water fraction was found for the annual and spring seasonal results but were lost for the summer and winter.

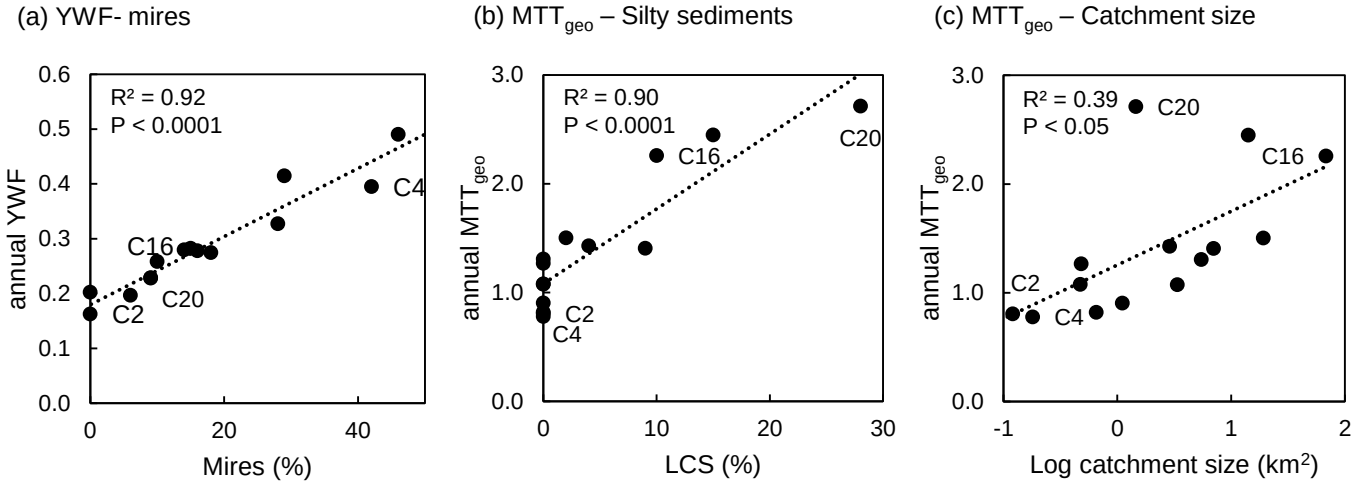

Figure 8: Catchment characteristics are important for travel times. The figure shows the annual averages: (a) the areal coverage of mires and the young water fraction (YWF), (b) areal coverage of silt and MTT_{geo}, and (c) catchment size and MTT_{geo}.

Table 6: Correlation matrix – young water fraction (YWF), geometric mean travel time (MTT_{geo}), and catchment characteristics. The catchment characteristics include the log catchment size, km^2 (Log C.-size), the areal coverage of mires, and the areal coverage of silt. The table includes annual (grey), winter (blue), spring (green), and summer (orange) results. Darker colours show |r| > 0.5 with the connected p-value according to [a] p<0.05 and [b] p>0.05.

	Winter season					Summer season				
	Log C.-size	**Mire (%)**	**Silt (%)**	**MTT_{geo}**	**YWF**	**Log C.-size**	**Mire (%)**	**Silt (%)**	**MTT_{geo}**	**YWF**
Log C.-size	1					1			0.91 [a]	
Mire (%)		1	0.92 [a]		0.64 [a]		1	0.80 [a]	-0.50 [b]	0.68 [a]
Silt (%)	0.58 [a]		1		0.58 [a]	0.58 [a]		1		0.58 [a]
MTT_{geo}	0.63 [b]	-0.51 [b]	0.90 [a]	1		0.55 [a]	-0.55 [a]	0.92 [a]	1	
YWF (%)		0.96 [a]		-0.53 [b]	1		0.95 [a]		-0.52 [b]	1
	Annual					Spring season				

4 Discussion

Particle tracking in the Mike SHE model provided valuable insights into the annual and seasonal mean travel times (MTT_{geo}) across the 14 Krycklan sub-catchments. The modelled MTT_{geo} and the young water fractions were strongly correlated to observed stream $\delta^{18}O_{winter}$ signatures, seasonal variation in $\delta^{18}O$, and base cation (BC) concentrations. This model validation suggests that particle tracking is a useful complementary tool to tracer-based studies of travel time, at least in snow-dominated catchments, areas with pronounced seasonality, and streams dominated by older groundwater (> four years). Overall, we found that soil type was the most important variable explaining MTT_{geo} and that mires are an important landscape feature regulating the young water fraction in spring (Fig.8).

4.1 Model assumptions and limitations of estimated travel times

Comparing the results from this modelling study to previous Krycklan investigations of MTT conducted in the C7 sub-catchment demonstrates that different model approaches have provided similar results. While our study suggested a MTT_{geo} of 1.1 years and a median of 0.8 years (Appendix, Table A1), Peralta-Tapia et al. (2016) calculated a MTT of 1.8 (minimum 0.8 and maximum 3.3) years using long-term isotopic data and a gamma transformation method. In another recent study using the Spatially distributed Tracer-Aided Rainfall-Runoff (STARR) model for the same stream, the median age was estimated to be 0.9 years (Ala-aho et al., 2017). The close agreement between the different studies strengthen the overall reliability of the results. However, like all modeling techniques, particle tracking in Mike SHE is associated with some uncertainties and limitations.

In contrast to the Mike SHE flow model, which estimates both the groundwater and overland flow pathways, the particle tracking model is restricted to the subsurface hydrological component. This is a limitation in the modelling approach as water reach streams as a mix of groundwater and overland flow. Therefore, to allow for actual MTT_{geo} estimates, we corrected the results by reducing the estimated MTT_{geo} using the overland flow from the flow model as a scaling factor. This uncertainty primarily affects the mire dominated sub-catchments that have a large fraction of overland flow, especially during the spring.

Another uncertainty related to the particle tracking model in Mike SHE is related to the travel time from the point of infiltration through the unsaturated soil horizons to the saturated groundwater. Due to technical limitations, this travel time cannot be accounted for in the particle tracking calculations. Particles are placed at the groundwater table proportionally to the groundwater recharge (Fig. 4). Therefore, the main fraction of particles introduced to the model occurs at high infiltration rates when the groundwater level is close to the soil surface. Under these conditions, the water has, in most cases, spent a relatively short time in the unsaturated zone. However, some particles are also introduced when the groundwater level is lower, such as early snowmelt or following extended dry periods. Under such conditions, the model uncertainty increase. In this context, the smallest potential uncertainty occurs in mires that seldom experience a groundwater table below one meter below the soil surface. The uncertainty becomes somewhat larger in the till areas where the unsaturated zone on average is above 1 m but can extend down to 3 m below the ground during low flow. C14 and the lower part of C16 are exceptions to these relatively shallow saturated conditions as a deep esker traverses the sub-catchments resulting in a groundwater level up to 10 m below the soil surface (Fig. 1). Accounting for the travel time from infiltration to recharge could impact the results and provide, especially for C14 and C16, longer MTT than if the groundwater level were at the same level throughout the whole catchment. This limitation primarily affects catchments with the longest MTTs and, therefore, does not seriously question the general pattern observed. The distance from the ground surface to the groundwater table is for most model cells much shorter than the distance to the nearest stream so

most of the transit time should be related to the groundwater flow rather than to percolation. Although water, especially during dry conditions, no doubt can spend considerable time in the unsaturated zone, it must also be acknowledged that this water volume is small compared to the groundwater inventory in the saturated zone so its impact on the average MTTs should be relatively small.

4.2 Seasonality of isotopic composition

Following the conceptual model (Fig. 2), patterns in stream isotopic signatures can be explained by seasonal changes in travel times. The modelling results show that all sub-catchments discharged the oldest water in winter, somewhat younger water in summer, and water of the youngest age in spring. When winter arrived, the main precipitation was snow resulting in that groundwater recharge effectively ceased, which caused an increasing proportion of old groundwater discharging into the streams (Fig. 6). In agreement with our conceptual model (Fig. 2), a strong negative correlation between winter MTT_{geo} and the isotopic stream signatures during winter baseflow was observed (Fig. 7a). At an average water age older than four years, it can be expected that the groundwater has reached full mixing. Hence, older water can no longer be accurately quantified using water isotopes only due to amplitude loss (Kirchner., 2016). These theoretical considerations strengthen the results of a winter MTT_{geo} between four and six years for the larger sub-catchments as their stream isotopic signatures were close to the long-term precipitation average and, therefore, should have reached complete mixing.

When snowmelt began in late April or early May, the MTTs consistently decreased in all sub-catchments. The fraction of young groundwater in different sub-catchments was well reflected in the change in the isotope signal (Fig. 7). For snowmelt in spring, the calculated young water fraction was used to evaluate the proportion of water reaching the stream through rapid pathways, including overland flow. It is well established that the difference in stream isotopic signature between winter baseflow and spring peak flow at snowmelt ($\Delta\delta^{18}O_{spring}$) is mechanistically linked to the amount of new water reaching the stream (Tetzlaff et al., 2009). In agreement with this, we found a strong statistical relationship between $\Delta\delta^{18}O_{spring}$ and the calculated young water fraction (Fig. 7c). These results are well in line with previous work in Krycklan using end-member mixing of new and old water in the same streams (Laudon et al., 2004, 2007, 2011).

Similar to the conditions in spring, the conceptual model predicted that the difference in stream isotopic signature between winter baseflow and summer flow, $\Delta\delta^{18}O_{summer}$, should be correlated to the young water fraction in summer, but with the opposite sign, due to isotopically heavier summer rains (Fig. 2). A larger inter-annual variation in precipitation and high ET likely caused the relationship to be less evident compared to the spring results as the snowmelt conditions are more consistent from year to year. However, although less evident than compared to the $\Delta\delta^{18}O_{spring}$, there was still a significant correlation between the average $\Delta\delta^{18}O_{summer}$ and the modelled young water fraction (Fig. 7e).

4.3 Controls of travel times on base cation concentrations

The annual and seasonal average BC concentrations were positively correlated with the MTT_{geo} (Fig. 7b, 7d, and 7f). Since the weathering rates were assumed to be kinetically controlled and hence related to the exposure time of water to minerals, spatial and temporal variability in BCs can be used as a relative indicator for transit time if the mineralogy remains comparatively homogenous (Erlandsson Lampa et al., 2020). However, reducing weathering to travel times may be an oversimplification as the rate is also affected by differences in mineralogy, particle size distributions and the chemical conditions in the groundwater. However,

previous research in the Krycklan catchment has suggested that the chemical composition of the local mineral soils is surprisingly homogeneous, even when comparing till and sorted sediments (Klaminder et al., 2011; Peralta-Tapia et al., 2015; Erlandsson et al., 2016; Lidman et al., 2016). Therefore, we did not expect mineralogical differences between soil types to significantly impact the release of cations. One exception, however, are peat deposits, which strongly affect the cation concentrations on a landscape scale. The effect of the peat was accounted for by adjusting the concentrations following Lidman et al. (2014). Differences in particle size distribution may be important because coarser soils will have less surface area per volume unit, allowing for less weathering. However, such soils can also be expected to have higher hydraulic conductivities, leading to higher flow velocities and, consequently, less time available for weathering. Therefore, differences in area-volume ratios between different soil types would not counteract the effect of travel times on the weathering, rather enhance it.

Despite arguments that can be made against the use of BCs as tracers, they still offer a complementary possibility to test the model performance (Abbott et al., 2016). As McDonnell and Beven (2014) emphasized, the inclusion of tracers in hydrological models is necessary to ensure that a model reproduces the speed of flow, which is an important parameter when assessing travel time distributions. For catchment-scale models, this could be an isotopic tracer or a solute transported with the water (Hooper et al., 1988; Seibert et al., 2003; Fenicia et al., 2010; Hrachowitz et al., 2013). Although neither the travel time distribution nor the kinetics of weathering is fully understood, the strong agreement between the calculated travel times and the observed stream water chemistry provides additional support that our modelling of these processes – and thus the entire system – was reasonable and consistent with the empirical data.

4.4 Mean travel times, young water fractions, and catchment characteristics

All sub-catchments showed similar synchronicity in the seasonal patterns in MTT_{geo} and young water fraction, but catchment characteristics influenced the magnitude of the seasonal patterns across the landscape. On a landscape level, the main causal mechanism determining the annual MTT_{geo} was the areal coverage of silt, which overshadowed the importance of other catchment characteristics (Fig. 8, Table 6). This finding stands in contrast to earlier studies in Krycklan by Peralta-Tapia et al. (2015) and Tiwari et al. (2017) that suggested that the groundwater travel times are nonlinearly linked to the catchment size. We found that the small silt dominated C20 catchment was a distinct outlier to such a scale-dependent pattern, indicating that catchment size may not be the primary factor determining the variability (Fig. 6). The reason is most likely that C20 is the only relatively small sub-catchment in the silt-dominated areas. Hence, the long travel times in C20 suggest that the groundwater flow velocity is slower than elsewhere in Krycklan, despite the fact that the average catchment slope is steeper than comparably sized sub-catchments in till areas (Table 1 and Fig. 1). Similarly, silt may also explain the long travel times at C14 and C16. Although C14 is smaller than C15, which mostly lacks silt, C14 still has a longer MTT_{geo}. In contrast, MTT_{geo} in C15 is much closer to C12 and C13, even though the C15 catchment is twice the size (Table 5). The results suggest that the critical difference between these sub-catchments and other sub-catchments is related to the soil hydraulic conductivity rather than the catchment size. The results further emphasize that one cannot assume that the travel time would increase with catchment size unless the distribution of different soils are comparable throughout the landscape.

The silt fraction effect is especially prominent in winter when the range in MTT_{geo} is between one and almost eight years. The seasonal MTT_{geo} change from winter to spring is also largest for the silt dominated catchments, with, for example, six years difference for C20 compared to two years for the similar-sized till dominated sub-catchment C6. These intra-annual variations can

also be linked to another landscape feature, namely the areal coverage of mires. Mires affected the young water fraction but only when new precipitation or snowmelt input into the system occurred in spring and summer. The lack of synchronicity between the response of mire and silt areas caused greater annual MTT_{geo} variation for sub-catchments with both features. For example, the MTT_{geo} for C4, dominated by mires, decreased from 1.5 years to 0.7 years from winter to spring. In contrast, winter MTT_{geo} for the C20 catchment dominated by silt was 7.7 years, which decreased to 1.5 years in spring. The results also show that groundwater recharge is affected by the soil frost in mires. For example, C4 showed more variations in its seasonal MTT_{geo}, although C2 (dominated by forest and till) and C4 (dominated by mires) had almost an equal annual MTT_{geo} (Table 5). In spring, the MTT_{geo} was shorter in C4 than in C2 due to surface runoff on the frozen mire, and in winter, the MTT_{geo} in C4 was longer than in C2 due to the lower recharge and displacement of older water during the spring. Besides the slightly higher specific discharge from mires (Karlsen et al. 2016), empirical-based studies suggest that the soil frost on mires causes a large fraction of overland flow (Laudon et al. 2007; 2011).

Earlier studies have demonstrated that fluxes of old groundwater are more stable throughout the year than younger groundwater showing a more variable temporal pattern (Rinaldo et al., 2011; van der Velde et al., 2015; Kaandrop et al., 2018). In our system, such a pattern can mechanistically be linked to till soils dominating most sub-catchments, where the groundwater response to precipitation events can be described by transmissivity feedback processes (Bishop, 1991), caused by the fact that the hydraulic conductivity increases exponentially towards the soil surface. When water infiltrates the ground, the water table rises and activates more conductive soil layers, resulting in rapid increases in the lateral flow. This implies that much of the water transport in till soil occurs relatively close to the surface, while the groundwater in deeper layers is more stagnant, which further explains the relatively short and consistent MTTs of till soils. Measurements of chlorofluorocarbons (CFCs) further support that deeper groundwater water transport in till soils in Krycklan is slow. Not far below the groundwater table CFCs have indicated that the groundwater can be several decades old, suggesting that most of the groundwater transport occurs close to the surface (Kolbe et al., 2020). Consistent with this explanation, silt dominated areas, that have more consistent hydrological conductive with soil depth, had much longer MTTs than comparatively sized sub-catchments underlain by till soils (Fig 6, Fig. 8 and Appendix Fig. A1).

5 Conclusions

The combination of stable water isotopes, stream water chemistry, and particle tracking provided a consistent picture of the hydrological functioning of a boreal catchment and what processes and factors are most important for regulating travel times and pathways. We identified specific landscape characteristics that impact the seasonal distribution of travel times by combining a distributed hydrological model with empirical observations from 14 nested sub-catchments. In the wake of a changing climate and intensified pressure from forestry and other types of land use, this study provides a useful baseline for assessing the intricate connections and feedbacks between hydrological and biogeochemical processes throughout the boreal landscape. Our results showed that water travel times could vary considerably on annual and seasonal scales between different types of catchments. This was mainly related to soil properties, with low conductivity silty sediments leading to the longest travel times on annual and seasonal timescales. In contrast, mires lead to increased fractions of young water, and hence shorter travel times, but mainly in spring when the soil was frozen. As a result of the lower groundwater recharge during the snowmelt, however, the MTTs in mires were, in turn, longer than in forests during the winter. In a warmer climate with reduced soil frost and decreased snowmelt input, we would expect the effect of mires to be reduced while the impact of till and silty sediment soils likely will remain relatively unaffected.

6 Data availability

Data from the Hydrological Research at Krycklan Catchment Study is available in Svartbergets open database (www.slu.se/Krycklan). The software (Mike SHE/Mike 11) is available at https://www.mikepoweredbydhi. com/

7 Author contribution

Elin Jutebring Sterte and Hjalmar Laudon were responsible for designing, conceptualizing, and evaluating results in collaboration with the other co-authors. Elin Jutebring Sterte and Emma Lindborg were responsible for numerical modelling. Elin Jutebring Sterte prepared the manuscript and figures. Elin Jutebring Sterte lead the writing of the paper with contributions from all co-authors.

8 Competing interests

The authors declare that they have no conflict of interest.

9 Acknowledgments

We like to thank the anonymous reviewers and the editor, Conrad Jackisch, for their time and effort, improving the quality of our work. Their combined constructive criticism has helped to refine the text and figures of this study. The authors are also thankful to the funding agency Svensk Kärnbränslehantering AB (SKB), the Danish Hydraulic Institute (DHI) for software access and expert consultation, and the crew of the Krycklan Catchment Study (KCS) funded by SITES (VR) for advice and data collection. KCS is funded by the Swedish University of Agricultural Sciences, Swedish Research Council (as part of the SITES network and project funds), FORMAS, Knut and Alice Wallenberg Foundation through Branch-Point and Future Siliviculture, Kempe foundation and, SKB. Data is available from the open Krycklan database (Laudon et al., 2013). Several individuals have also helped with the creation of this work. Special acknowledgment goes to Patrik Vidstrand (SKB) for bedrock properties consultation, Jan-Olof Selroos (SKB) for constructive comments and criticism, Hanna Corell (DHI) for initial particle release consultation, and Anders Lindblom (SKB) with the design of Fig. 1.

References

Abbott, B. W., Baranov, V., Mendoza-Lera, C., Nikolakopoulou, M., Harjung, A., Kolbe, T., Balasubramanian, M. N., Vaessen, T. N., Ciocca, F., Campeau, A., Wallin, M. B., Romeijn, P., Antonelli, M., Gonçalves, J., Datry, T., Laverman, A. M., de Dreuzy, J.-R., Hannah, D. M., Krause, S., Oldham, C. and Pinay, G.: Using multi-tracer inference to move beyond single-catchment ecohydrology, Earth-Science Rev., 160, 19–42, doi:https://doi.org/10.1016/j.earscirev.2016.06.014, 2016.

Ala-aho, P., Tetzlaff, D., McNamara, J. P., Laudon, H., and Soulsby, C.: Using isotopes to constrain water flux and age estimates in snow-influenced catchments using the STARR (Spatially distributed Tracer-Aided Rainfall–Runoff) model. Hydrology and Earth System Sciences, 21(10), 5089–5110, 2017.

Ameli, A. A., Amvrosiadi, N., Grabs, T., Laudon, H., Creed, I. F., McDonnell, J. J., and Bishop, K.: Hillslope permeability architecture controls on subsurface transit time distribution and flow paths, J. Hydrol., 543, 17–30, https://doi.org/10.1016/j.jhydrol.2016.04.071, 2016.

Aubin, I., Boisvert-Marsh, L., Kebli, H., McKenney, D., Pedlar, J., Lawrence, K., Hogg, E. H., Boulanger, Y., Gauthier, S., and Ste-Marie, C.: Tree vulnerability to climate change: improving exposure-based assessments using traits as indicators of sensitivity. Ecosphere 9(2):e02108. 10.1002/ecs2.2108, 2018.

Barnett, T. P., Adam, J. C., and Lettenmaier, D. P.: Potential impacts of a warming climate on water availability in snow-dominated regions. Nature, 438, 303. Retrieved from http://dx.doi.org/10.1038/nature04141, 2005.

Birkel, C., Geris, J., Molina, M. J., Mendez, C., Arce, R., Dick, J., et al.: Hydroclimatic controls on non-stationary stream water ages in humid tropical catchments, J. Hydrol., 542, 231–240, https://doi.org/10.1016/j.jhydrol.2016.09.006, 2016.

Bishop, K.H.: Episodic increases in stream acidity, catchment flow pathways and hydrograph separation. PhD Thesis, University of Cambridge, 246 pp, 1991.

Bishop, K., Seibert, J., Nyberg, L., and Rodhe, A.: Water storage in a till catchment. II: Implications of transmissivity feedback for flow paths and turnover times. Hydrological Processes, 25(25), 3950–3959. https://doi.org/10.1002/hyp.8355, 2011.

Bjerklie, D. M., Lawrence Dingman, S., Vorosmarty, C. J., Bolster, C. H., and Congalton, R.G.: Evaluating the potential for measuring river discharge from space. J. Hydrol. 278, 17–38. https://doi.org/https://doi.org/10.1016/S0022-1694(03)00129-X, 2003.

Bosson, E., Gustafsson, L.-G., and Sassner, M.: Numerical modelling of surface hydrology and near-surface hydrogeology at Forsmark. Stockholm, 2008.

Bosson, E., Sassner, M., Sabel, U., and Gustafsson, L.-G.: Modelling of present and future hydrology and solute transport at Forsmark. Stockholm, 2010.

Bosson, E., Selroos, J.-O., Stigsson, M., Gustafsson, L.-G., and Destouni, G.: Exchange and pathways of deep and shallow groundwater in different climate and permafrost conditions using the Forsmark site, Sweden, as an example catchment. Hydrogeology Journal, 21(1), 225–237. https://doi.org/10.1007/s10040-012-0906-7, 2013.

Botter, G., Bertuzzo, E., and Rinaldo, A.: Transport in the hydrologic response: Travel time distributions, soil moisture dynamics, and the old water paradox, Water Resour. Res., 46, https://doi.org/10.1029/2009WR008371, 2010.

Brirhet, H., and Benaabidate, L.: Comparison Of Two Hydrological Models (Lumped And Distributed) Over A Pilot Area Of The Issen Watershed In The Souss Basin, Morocco. European Scientific Journal, 12(18), 2016.

Burns, D. A., Plummer, L. N., McDonnell, J. J., Busenberg, E., Casile, G. C., Kendall, C., et al.: The Geochemical Evolution of Riparian Ground Water in a Forested Piedmont Catchment. Groundwater, 41(7), 913–925. https://doi.org/10.1111/j.1745-6584.2003.tb02434.x, 2003.

Danesh-Yazdi, M., Foufoula-Georgiou, E., Karwan, D. L., and Botter, G.: Inferring changes in water cycle dynamics of intensively managed landscapes via the theory of time-variant travel time distributions. Water Resources Research, 52(10), 7593–7614. https://doi.org/10.1002/2016WR019091, 2016.

Destouni, G., Simic, E. and Graham, W.: On the applicability of analytical methods for estimating solute travel time statistics in nonuniform groundwater flow, Water Resour. Res., 37(9), 2303–2308, doi:10.1029/2001WR000348, 2001.

Erlandsson, M., Oelkers, E. H., Bishop, K., Sverdrup, H., Belyazid, S., Ledesma, J. L. J., and Köhler, S. J.: Spatial and temporal variations of base cation release from chemical weathering on a hillslope scale. Chemical Geology, 441, 1–13. https://doi.org/10.1016/j.chemgeo.2016.08.008, 2016.

Erlandsson Lampa, M., Sverdrup, H.U., Bishop, K.H., Belyazid, S., Ameli, A., Köhler, S.J.: Catchment export of base cations: 660 improved mineral dissolution kinetics influence the role of water transit time. SOIL 6, 231–244. https://doi.org/10.5194/soil-6-231-2020, 2020.

Fenicia, F., Wrede, S., Kavetski, D., Pfister, L., Hoffmann, L., Savenije, H. H. G., and McDonnell, J. J.: Assessing the impact of mixing assumptions on the estimation of streamwater mean residence time. Hydrological Processes, 24(12), 1730–1741. https://doi.org/10.1002/hyp.7595, 2010.

von Freyberg, J., Allen, S. T., Seeger, S., Weiler, M., and Kirchner, J. W.: Sensitivity of young water fractions to hydro-climatic forcing and landscape properties across 22~Swiss catchments. Hydrology and Earth System Sciences, 22(7), 3841–3861. https://doi.org/10.5194/hess-22-3841-2018, 2018.

Frisbee, M. D., Phillips, F. M., Campbell, A. R., Liu, F., and Sanchez, S. A.: Streamflow generation in a large, alpine watershed in the southern Rocky Mountains of Colorado: Is streamflow generation simply the aggregation of hillslope runoff responses? Water Resources Research, 47(6). https://doi.org/10.1029/2010WR009391, 2011.

Goller, R., Wilcke, W., Leng, M. J., Tobschall, H. J., Wagner, K., Valarezo, C., and Zech, W.: Tracing water paths through small catchments under a tropical montane rain forest in south Ecuador by an oxygen isotope approach. Journal of Hydrology, 308(1–4), 67–80. https://doi.org/10.1016/J.JHYDROL.2004.10.022, 2005.

Graham, D. N., and Butts, M. B.: Flexible Integrated Watershed Modeling with MIKE SHE. Watershed Models, (September), 245–272. https://doi.org/10.1201/9781420037432.ch10, 2005.

Harman, C. J.: Time-variable transit time distributions and transport: Theory and application to storage-dependent transport of chloride in a watershed. Water Resources Research, 51(1), 1–30. https://doi.org/10.1002/2014WR015707, 2015.

Heidbüchel, I., Troch, P. A., and Lyon, S. W.: Separating physical and meteorological controls of variable transit times in zero-order catchments, Water Resour. Res., 49, 7644–7657, https://doi.org/10.1002/2012WR013149, 2013.

Heidbüchel, I., Troch, P. A., Lyon, S. W., and Weiler, M.: The master transit time distribution of variable flow systems, Water Resour. Res., 48, https://doi.org/10.1029/2011WR011293, 2012.

Hooper, R. P., Stone, A., Christophersen, N., de Grosbois, E., and Seip, H. M.: Assessing the Birkenes Model of stream acidification using a multisignal calibration methodology. Water Resources Research, 24(8), 1308–1316. https://doi.org/10.1029/WR024i008p01308, 1988.

Hrachowitz, M., Benettin, P., van Breukelen, B.M., Fovet, O., Howden, N.J., Ruiz, L., van der Velde, Y. and Wade, A.J.: Transit times—the link between hydrology and water quality at the catchment scale. WIREs Water, 3: 629-657. doi:10.1002/wat2.1155, 2016.

Hrachowitz, M., Fovet, O., Ruiz, L., and Savenije, H. H. G.: Transit time distributions, legacy contamination and variability in biogeochemical 1/fα scaling: how are hydrological response dynamics linked to water quality at the catchment scale? Hydrol. Process. 29, 5241–5256. https://doi.org/10.1002/hyp.10546, 2015.

Hrachowitz, M., Savenije, H., Bogaard, T. A., Tetzlaff, D., and Soulsby, C.: What can flux tracking teach us about water age distribution patterns and their temporal dynamics? Hydrology and Earth System Sciences, 17(2), 533–564. https://doi.org/10.5194/hess-17-533-2013, 2013.

Hrachowitz, M., Soulsby, C., Tetzlaff, D., Malcolm, I. A., and Schoups, G.: Gamma distribution models for transit time estimation in catchments: Physical interpretation of parameters and implications for time-variant transit time assessment, Water Resour. Res., https://doi.org/10.1029/2010WR009148, 2010.

Ivarsson, H., and Johnsson, T.: Stratigraphy of the Quaternary deposits in the Nyänges drainage area, within the Svartbergets forest experimental area and a general geomorphological description of the Vindeln region. Vartbergets and Kulbäckslidens Research Parks Stencil Series, 1988.

Jian, J., Ryu, D., Costelloe, J.F., and Su, C.-H.: Towards hydrological model calibration using river level measurements. J. Hydrol. Reg. Stud. 10, 95–109. https://doi.org/https://doi.org/10.1016/j.ejrh.2016.12.085, 2017.

Joyce, S., Simpson, T., Hartley, L., Applegate, D., Hoek, J., Jackson, P., and Swan, D.: Groundwater flow modelling of periods with temperate climate conditions – Forsmark R-09-20. Stockholm, 2010.

Jutebring Sterte, E., Johansson, E., Sjöberg, Y., Huseby Karlsen, R., and Laudon, H.: Groundwater-surface water interactions across scales in a boreal landscape investigated using a numerical modelling approach. Journal of Hydrology, 560, 184–201. https://doi.org/10.1016/J.JHYDROL.2018.03.011, 2018.

Kaandorp, V. P., de Louw, P. G. B., van der Velde, Y., and Broers, H. P.: Transient Groundwater Travel Time Distributions and Age-Ranked Storage-Discharge Relationships of Three Lowland Catchments. Water Resources Research, 54, 4519– 4536. https://doi.org/10.1029/2017WR022461, 2018.

Karlsen, R. H., Grabs, T., Bishop, K., Buffam, I., Laudon, H., and Seibert, J.: Landscape controls on spatiotemporal discharge variability in a boreal catchment. Water Resources Research, 52(8), 6541–6556. https://doi.org/10.1002/2016WR019186, 2016.

Kirchner, J. W.: Aggregation in environmental systems -- Part~1: Seasonal tracer cycles quantify young water fractions, but not mean transit times, in spatially heterogeneous catchments. Hydrology and Earth System Sciences, 20(1), 279–297. https://doi.org/10.5194/hess-20-279-2016, 2016.

Klaminder, J., Grip, H., Morth, C.-M., and Laudon, H.: Carbon mineralization and pyrite oxidation in groundwater: Importance for silicate weathering in boreal forest soils and stream base-flow chemistry. Applied Geochemistry, 26(3), 319–324. https://doi.org/10.1016/j.apgeochem.2010.12.005, 2011.

Klaus, J., Zehe, E., Elsner, M., Külls, C., and McDonnell, J. J.: Macropore flow of old water revisited: experimental insights from a tile-drained hillslope, Hydrol. Earth Syst. Sci., 17, 103–118, https://doi.org/10.5194/hess-17-103-2013, 2013.

Kolbe, T, Marçais, J, de Dreuzy, J-R, Labasque, T, Bishop, K.: Lagged rejuvenation of groundwater indicates internal flow structures and hydrological connectivity. Hydrological Processes; 34: 2176– 2189. https://doi.org/10.1002/hyp.13753, 2020.

Kralik, M.: How to Estimate Mean Residence Times of Groundwater. Procedia Earth and Planetary Science, 13, 301–306. https://doi.org/10.1016/J.PROEPS.2015.07.070, 2015.

Kristensen, K. J. and S.E. Jensen.: A model for estimating actual evapotranspiration from potential evapotranspiration. Royal Veterinary and Agricultural University, Nordic Hydrology 6, pp. 170-188, 1975.

Laudon, H., Berggren, M., Ågren, A. et al.: Patterns and Dynamics of Dissolved Organic Carbon (DOC) in Boreal Streams: The Role of Processes, Connectivity, and Scaling. Ecosystems 14, 880–893. https://doi.org/10.1007/s10021-011-9452-8, 2011.

Laudon, H., Seibert, J., Köhler, S., and Bishop, K.: Hydrological flow paths during snowmelt: Congruence between hydrometric measurements and oxygen 18 in meltwater, soil water, and runoff, Water Resour. Res., 40, W03102, doi:10.1029/2003WR002455., 2004.

Laudon, H., Sjöblom, V., Buffam, I., Seibert, J., and Mörth, M.: The role of catchment scale and landscape characteristics for runoff generation of boreal streams. Journal of Hydrology 344 (3-4), 198-209, 2007.

Laudon, H. and Sponseller, R.A.: How landscape organization and scale shape catchment hydrology and biogeochemistry: insights from a long-term catchment study. WIREs Water, 5: e1265. doi:10.1002/wat2.1265, 2018.

Laudon, H., Taberman, I., Ågren, A., Futter, M., Ottosson-Löfvenius, M., and Bishop, K.: The Krycklan Catchment Study - A flagship infrastructure for hydrology, biogeochemistry, and climate research in the boreal landscape. Water Resources Research, 49(10), 7154–7158. https://doi.org/10.1002/wrcr.20520, 2013.

Leach, J. A., and Laudon, H.: Headwater lakes and their influence on downstream discharge. Limnology and Oceanography Letters, 4(4), 105–112. https://doi.org/10.1002/lol2.10110, 2019.

Ledesma, J. L. J., Grabs, T., Futter, M. N., Bishop, K. H., Laudon, H., and Köhler, S. J.: Riparian zone control on base cation concentration in boreal streams. Biogeosciences, 10(6), 3849–3868. https://doi.org/10.5194/bg-10-3849-2013, 2013.

Ledesma, J. L. J., Futter, M. N., Blackburn, M., Lidman, F., Grabs, T., Sponseller, R. A., et al.: Towards an Improved Conceptualization of Riparian Zones in Boreal Forest Headwaters. Ecosystems, 21(2), 297–315. https://doi.org/10.1007/s10021-017-0149-5, 2018.

Li, C., Liu, J., Yu, F., Tian, J., Wang, Y., and Qiu, Q.: Hydrological Model Calibration in Data-Limited Catchments Using Non-Continuous Data Series with Different Lengths, 2018.

Lidman, F., Boily, Å., Laudon, and H., Köhler, S.J.: From soil water to surface water - how the riparian zone controls element transport from a boreal forest to a stream. Biogeosciences 14, 3001–3014. https://doi.org/10.5194/bg-14-3001-2017, 2017.

Lidman, F., Köhler, S. J., Morth, C.-M., and Laudon, H.: Metal transport in the boreal landscape - the role of wetlands and the affinity for organic matter. Environmental Science & Technology. https://doi.org/10.1021/es4045506, 2014.

Lidman, F., Peralta-Tapia, A., Vesterlund, A., and Laudon, H.: 234U/238U in a boreal stream network - Relationship to hydrological events, groundwater and scale. Chemical Geology. https://doi.org/10.1016/j.chemgeo.2015.11.014, 2016.

Lin, H.: Earth's Critical Zone and hydropedology: concepts, characteristics, and advances. Hydrol. Earth Syst. Sci. 14, 25–45. https://doi.org/10.5194/hess-14-25-2010, 2010.

Lutz, S. R., Krieg, R., Müller, C., Zink, M., Knöller, K., Samaniego, L., and Merz, R.: Spatial Patterns of Water Age: Using Young Water Fractions to Improve the Characterization of Transit Times in Contrasting Catchments. Water Resources Research, 54(7), 4767–4784. https://doi.org/10.1029/2017WR022216, 2018.

Lyon, S.W., Ploum, S.W., van der Velde, Y., Rocher-Ros, G., Mörth, C.-M., and Giesler, R.: Lessons learned from monitoring the stable water isotopic variability in precipitation and streamflow across a snow-dominated subarctic catchment. Arctic, Antarct. Alp. Res. 50, e1454778. https://doi.org/10.1080/15230430.2018.1454778, 2018.

Massoudieh, A., Sharifi, S. and Solomon, D. K.: Bayesian evaluation of groundwater age distribution using radioactive tracers and anthropogenic chemicals, Water Resour. Res., 48(9), doi:https://doi.org/10.1029/2012WR011815, 2012.

Massoudieh, A., Dentz, M. and Alikhani, J.: A spatial Markov model for the evolution of the joint distribution of groundwater age, arrival time, and velocity in heterogeneous media, Water Resour. Res., 53(7), 5495–5515, doi:https://doi.org/10.1002/2017WR020578, 2017.

Maulé, C. P., and Stein, J.: Hydrologic Flow Path Definition and Partitioning of Spring Meltwater. Water Resources Research, 26(12), 2959–2970. https://doi.org/10.1029/WR026i012p02959, 1990.

McDonnell, J. J., and Beven, K.: Debates—The future of hydrological sciences: A (common) path forward? A call to action aimed at understanding velocities, celerities and residence time distributions of the headwater hydrograph. Water Resources Research, 50(6), 5342–5350. https://doi.org/10.1002/2013WR015141, 2014.

McDonnell, J. J., McGuire, K., Aggarwal, P., Beven, K. J., Biondi, D., Destouni, G., et al.: How old is streamwater? Open questions in catchment travel time conceptualization, modelling and analysis. Hydrological Processes, 24(12), 1745–1754. https://doi.org/10.1002/hyp.7796, 2010.

McGuire, K. J., and McDonnell, J. J.: A review and evaluation of catchment transit time modeling. Journal of Hydrology. 330: 543-563, https://doi.org/10.1016/j.jhydrol.2006.04.020, 2006.

McGuire, K. J., McDonnell, J. J., Weiler, M., Kendall, C., McGlynn, B. L., Welker, J. M., and Seibert, J.: The role of topography on catchment-scale water residence time. Water Resources Research, 41(5). https://doi.org/10.1029/2004WR003657, 2005.

McGuire, K.J., Weiler, M., and McDonnell, J.J.: Integrating tracer experiments with modeling to assess runoff processes and water transit times. Adv. Water Resour. 30, 824–837. https://doi.org/https://doi.org/10.1016/j.advwatres.2006.07.004, 2007.

Morris, D. A., and Johnson, A. I.: Summary of hydrologic and physical properties of rock and soil materials, as analyzed by the hydrologic laboratory of the U.S. Geological Survey, 1948-60. Water Supply Paper, 42. Retrieved from http://pubs.er.usgs.gov/publication/wsp1839D, 1967.

Nyberg, L.: Water flow path interactions with soil hydraulic properties in till soil at Gårdsjön, Sweden. Journal of Hydrology, 170(1), 255–275. https://doi.org/https://doi.org/10.1016/0022-1694(94)02667-Z, 1995.

Peralta-Tapia, A., Soulsby, C., Tetzlaff, D., Sponseller, R., Bishop, K., and Laudon, H.: Hydroclimatic influences on non-stationary travel time distributions in a boreal headwater catchment. Journal of Hydrology. https://doi.org/10.1016/j.jhydrol.2016.01.079, 2016.

Peralta-Tapia, A., Sponseller, R. A., Ågren, A., Tetzlaff, D., Soulsby, C., and Laudon, H.: Scale-dependent groundwater contributions influence patterns of winter baseflow stream chemistry in boreal catchments. Journal of Geophysical Research: Biogeosciences, 120(5), 847–858. https://doi.org/10.1002/2014JG002878, 2015.

Peralta-Tapia, A., Sponseller, R. A., Tetzlaff, D., Soulsby, C., and Laudon, H.: Connecting precipitation inputs and soil flow pathways to stream water in contrasting boreal catchments. Hydrological Processes, 29(16), 3546–3555. https://doi.org/10.1002/hyp.10300, 2014.

Peters, N.E., Burns, D.A. and Aulenbach, B.T.: Evaluation of High-Frequency Mean Streamwater Transit-Time Estimates Using Groundwater Age and Dissolved Silica Concentrations in a Small Forested Watershed. Aquat Geochem 20, 183–202. https://doi.org/10.1007/s10498-013-9207-6, 2014.

Rahim, B. E. A., Yusoff, I., Jafri, A. M., Othman, Z. and Abdul Ghani, A.: Application of MIKE SHE modelling system to set up a detailed water balance computation, Water Environ. J., 26(4), 490–503, doi:https: //doi.org/10.1111/j.1747-6593.2012.00309.x, 2012.

Rinaldo, A., Beven, K. J., Bertuzzo, E., Nicotina, L., Davies, J., Fiori, A., Russo, D., and Botter, G.: Catchment travel time distributions and water flow in soils, Water Resour. Res., 47, W07537, doi:10.1029/2011WR010478, 2011.

Rodhe, A., Nyberg, L., and Bishop, K.: Transit Times for Water in a Small Till Catchment from a Step Shift in the Oxygen 18 Content of the Water Input. Water Resources Research, 32(12), 3497–3511. https://doi.org/10.1029/95WR01806, 1996.

Seibert, J., Grabs, T., Köhler, S., Laudon, H., Winterdahl, M., and Bishop, K.:. Linking soil- and stream-water chemistry based on a Riparian Flow-Concentration Integration Model. Hydrology and Earth System Sciences, 13(12), 2287–2297. https://doi.org/10.5194/hess-13-2287-2009, 2009.

Seibert, J., Rodhe, A., and Bishop, K.: Simulating interactions between saturated and unsaturated storage in a conceptual runoff model. Hydrological Processes, 17(2), 379–390. https://doi.org/10.1002/hyp.1130, 2003.

Sishodia, R. P., Shukla, S., Graham, W. D., Wani, S. P., Jones, J. W. and Heaney, J.: Current and future groundwater withdrawals: Effects, management and energy policy options for a semi-arid Indian watershed, Adv. Water Resour., 110, 459–475, doi:https://doi.org/10.1016/j.advwatres.2017.05.014, 2017.

Soltani, S. S.: Hydrological Transport in Shallow Catchments: tracer discharge, travel time and water age. KTH Royal Institute of Technology, 2017.

Spence, C., Guan, X.J., and Phillips, R.: The Hydrological Functions of a Boreal Wetland. Wetlands 31, 75–85. https://doi.org/10.1007/s13157-010-0123-x, 2011.

Spence, C., and Phillips, R.W.: Refining understanding of hydrological connectivity in a boreal catchment. Hydrol. Process. 29, 3491–3503. https://doi.org/10.1002/hyp.10270, 2015.

Sprenger, M., Tetzlaff, D., Buttle, J., Laudon, H., and Soulsby, C.: Water ages in the critical zone of long-term experimental sites in northern latitudes. Hydrology and Earth System Sciences Discussions, 1–26, 2018.

Stockinger, M. P., Bogena, H. R., Lücke, A., Stumpp, C., and Vereecken, H.: Time-variability of the fraction of young water in a small headwater catchment. Hydrology and Earth System Sciences Discussions, 2019, 1–25. https://doi.org/10.5194/hess-2018-604, 2019.

Taagepera, R.: Making Social Sciences More Scientific: The Need for Predictive Models. Oxford: Oxford University Press. https://doi.org/10.1093/acprof:oso/9780199534661.001.0001, 2008.

Tetzlaff, D, Buttle, J, Carey, SK, McGuire, K, Laudon, H, and Soulsby, C.: Tracer-based assessment of flow paths, storage and runoff generation in northern catchments: a review. Hydrol. Process., 29, 3475– 3490. doi: 10.1002/hyp.10412, 2015.

Tetzlaff, D., Seibert, J., McGuire, K.J., Laudon, H., Burns, D.A., Dunn, S.M. and Soulsby, C.: How does landscape structure influence catchment transit time across different geomorphic provinces?. Hydrol. Process., 23: 945-953. doi:10.1002/hyp.7240, 2009.

Tetzlaff, D., and Soulsby, C.: Sources of baseflow in larger catchments – Using tracers to develop a holistic understanding of runoff generation. Journal of Hydrology, 359(3), 287–302, 2008.

Tiwari, T., Buffam, I., Sponseller, R. A., and Laudon, H.: Inferring scale-dependent processes influencing stream water biogeochemistry from headwater to sea. Limnology and Oceanography. https://doi.org/10.1002/lno.10738, 2017.

Tremblay, L., Larocque, M., Anctil, F., and Rivard C.: Teleconnections and interannual variability in Canadian groundwater levels. Journal of Hydrology. https://doi.org/10.1016/j.jhydrol.2011.09.013, 2011.

Uhlenbrook, S., Frey, M., Leibundgut, C., and Maloszewski, P.: Hydrograph separations in a mesoscale mountainous basin at event and seasonal timescales. Water Resources Research, 38(6), 14–31. https://doi.org/10.1029/2001WR000938, 2002.

Unlu, E. and Faller, J.F. (2001), Geometric mean vs. Arithmetic mean in extrusion residence time studies. Polym Eng Sci, 41: 743-751. https://doi.org/10.1002/pen.10770

van der Velde, Y, Heidbüchel, I, Lyon, SW, Nyberg, L, Rodhe, A, Bishop, K, and Troch, PA.: Consequences of mixing assumptions for time-variable travel time distributions. Hydrol. Process., 29, 3460– 3474. doi: 10.1002/hyp.10372, 2015.

van der Velde, Y., Torfs, P. J. J. F., Zee, S. E. A. T. M., and Uijlenhoet, R.: Quantifying catchment-scale mixing and its effect on time-varying travel time distributions. Water Resources Research, 48(6). https://doi.org/10.1029/2011WR011310, 2012.

Wang, L., H. van Meerveld, J., and Seibert, J.; When should stream water be sampled to be most informative for event-based, multi-criteria model calibration?. Hydrology Research; 48 (6): 1566–1584. doi: https://doi.org/10.2166/nh.2017.197, 2017.

Wang, S., Zhang, Z., Sun, G., Strauss, P., Guo, J., Tang, Y. and Yao, A.: Multi-site calibration, validation, and sensitivity analysis of the MIKE SHE Model for a large watershed in northern China, Hydrol. Earth Syst. Sci., 16(12), 4621–4632, doi:10.5194/hess-16-4621-2012, 2012.

Wolock, D. M., Fan, J., and Lawrence, G. B.: Effects of basin size on low-flow stream chemistry and subsurface contact time in the Neversink River watershed, New York. Hydrological Processes, 11, 1273–1286. https://doi.org/10.1002/(SICI)1099-1085(199707)11:9<1273::AID-HYP557>3.0.CO;2-S, 1997.

Wijesekara, G. N., Farjad, B., Gupta, A., Qiao, Y., Delaney, P. and Marceau, D. J.: A Comprehensive Land-Use/Hydrological Modeling System for Scenario Simulations in the Elbow River Watershed, Alberta, Canada, Environ. Manage., 53(2), 357–381, doi:10.1007/s00267-013-0220-8, 2014.

Yang, J., Heidbüchel, I., Musolff, A., Reinstorf, F., and Fleckenstein, J. H.: Exploring the dynamics of transit times and subsurface mixing in a small agricultural catchment, Water Resour. Res., https://doi.org/10.1002/2017WR021896, 2018.

Zhang, C., Zhang, S.: A robust-symmetric mean: A new way of mean calculation for environmental data. GeoJournal 40, 209–212. https://doi.org/10.1007/BF00222547, 1996.

Zimmer, M. A., Bailey, S. W., McGuire, K. J., and Bullen, T. D.: Fine scale variations of surface water chemistry in an ephemeral to perennial drainage network. Hydrological Processes, 27(24), 3438–3451. https://doi.org/10.1002/hyp.9449, 2012.

Appendix

In the Appendix, statistical measurements for particle tracking and isotope data are further explained, used in e.g., table 5 and table A1. The statistics used in this study include arithmetic mean (Eq. A1), geometric mean (Eq. A2), standard deviation (Eq. A3), standard error of the mean (Eq. A4). The isotopic signature of $\delta^{18}O$ has been calculated as Eq. A5.

$$\text{Arithmetic mean of the travel time distribution} = \left(\frac{1}{\mathrm{n}}\right)\sum_{i=1}^{n} ai \quad \text{(Eq. A1)}$$

$$\text{Geometric mean of the travel time distribution} = 10^{\left(\frac{1}{\mathrm{n}}\right)\sum_{i=1}^{n}\log(ai)} \quad \text{(Eq. A2)}$$

$$\mathrm{SD} = \text{standard deviation} = \sqrt{\frac{\sum(ai-aMTT)^2}{N}} \quad \text{(Eq. A3)}$$

$$\mathrm{SEM} = \text{standard error of the mean} = \frac{SD}{\sqrt{n}} \quad \text{(Eq. A4)}$$

$$\delta = \left(\frac{R_{sample}}{R_{standard}} - 1\right) ‰, \text{ whereas R} = \frac{18O}{16O} \quad \text{(Eq. A5)}$$

whereas: ai= data set values, n=number of values.

The Appendix also includes an extended version of table 5 and Fig. 6, including all sub-catchments (Table A1 and Fig. A1). The figure shows the fraction of different age groups to the streams of the sub-catchment in Krycklan annually. The figure shows both the groundwater fraction (age fraction calculated using the particle tracking results) and the fraction of simulated direct runoff. The table shows more statistical information regarding the travel time distribution, including the Skew, SD, and SEM.

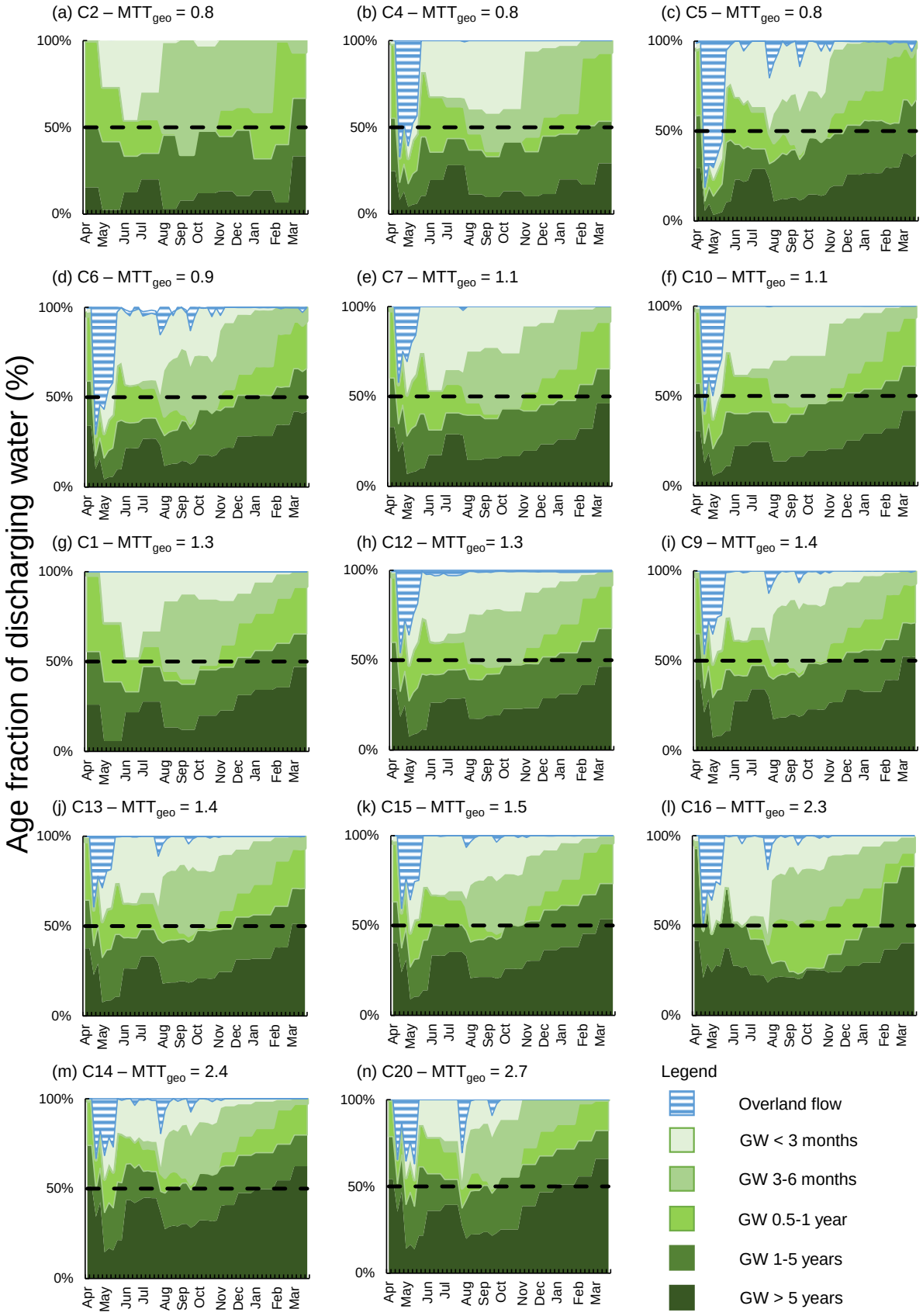

875

Figure A1: Age fraction of water discharging to the streams of Krycklan, in increasing annual geometric mean travel time, MTT$_{geo}$ (up left to down right). The black vertical line shows the 50 % mark for visual aid. All charts begin in spring (late March/early April) and end in winter (early March).

Table A1: Extended version of Table 5 - Annual and seasonal (winter, spring, and summer) travel time results.
The table includes the travel time results based on particle tracking ***before*** taking the overland flow into account. The results include arithmetic mean (A), median (M), geometric mean (Geo), skew, standard deviation (SD), and standard error of the mean (SEM).

	Annual						Season - Winter					
	A	M	Geo	Skew	SD	SEM	A	M	Geo	Skew	SD	SEM
unit	year	year	year	-	-	-	year	year	year	-	-	-
C1	10.1	1.0	1.3	4.1	27	0.4	18.8	1.4	3.0	2.7	36	1.2
C2	2.2	0.9	0.8	5.0	5	0.2	2.7	0.7	1.2	2.4	4	0.5
C4	7.7	0.8	1.0	7.5	34	1.0	10.5	1.1	1.5	6.6	42	2.7
C5	15.2	1.0	1.3	6.4	61	1.0	30.4	1.4	2.9	4.1	84	3.2
C6	13.7	0.8	1.2	6.8	51	0.6	25.9	1.4	2.8	4.6	69	1.8
C7	8.0	0.8	1.2	7.4	25	0.4	13.2	1.3	2.2	5.6	32	1.1
C9	13.2	1.0	1.6	6.7	38	0.3	21.6	1.6	3.4	5.0	47	0.7
C10	10.9	0.9	1.2	6.4	35	0.2	16.5	1.4	2.5	4.5	40	0.6
C12	11.9	1.0	1.4	5.5	33	0.2	17.6	1.0	2.8	4.0	37	0.4
C13	13.3	1.0	1.5	8.0	43	0.2	21.6	1.6	3.3	6.4	53	0.5
C14	18.3	1.9	2.7	7.8	54	0.2	26.4	6.6	5.6	6.8	60	0.4
C15	14.3	1.0	1.7	8.7	43	0.1	21.9	2.4	3.8	6.7	49	0.3
C16	17.4	1.7	2.5	8.5	50	0.2	25.3	6.7	5.3	7.3	57	0.2
C20	21.9	1.8	3.1	6.0	52	0.6	32.9	9.7	7.7	5.8	55	1.1

	Season - Spring						Season - Summer					
	A	M	Geo	Skew	SD	SEM	A	M	Geo	Skew	SD	SEM
unit	year	year	year	-	-	-	year	year	year	-	-	-
C1	5.2	1.0	1.0	6.8	19	0.5	8.4	0.4	0.9	4.5	25	0.8
C2	1.6	1.0	0.7	6.1	3	0.2	2.7	0.4	0.7	4.2	8	0.6
C4	5.7	0.3	1.2	10.8	27	1.5	9.1	0.4	0.7	6.1	39	2.0
C5	9.9	1.0	1.2	9.3	50	1.5	11.3	0.4	0.8	7.6	52	1.7
C6	9.1	0.9	1.0	9.5	45	1.0	9.9	0.4	0.8	8.2	42	1.0
C7	5.5	1.0	1.1	11.2	19	0.6	7.5	0.4	0.9	7.5	27	0.8
C9	8.2	1.0	1.3	10.8	31	0.4	11.2	0.8	1.2	7.0	34	0.5
C10	8.0	1.0	1.1	8.2	32	0.4	9.0	0.4	0.9	6.3	31	0.4
C12	8.2	1.0	1.2	7.6	29	0.3	10.2	0.8	1.1	5.3	29	0.3
C13	7.8	1.0	1.2	10.8	30	0.3	12.5	0.8	1.2	8.8	45	0.4
C14	12.2	1.6	2.1	10.6	45	0.3	16.3	1.1	1.8	7.9	54	0.4
C15	9.2	1.0	1.2	11.4	34	0.2	12.4	0.9	1.2	9.2	41	0.2
C16	11.4	1.1	1.7	11.0	40	0.1	15.6	1.0	1.8	8.9	48	0.2
C20	12.2	1.9	2.6	10.5	39	0.8	20.4	1.0	1.6	5.4	59	1.3